AWARD NUMBER: W81XWH-20-1-0327

TITLE: Evaluation of Adipose-Derived Stem Cells and Metformin Combination Therapy for Radiation Fibrosis

PRINCIPAL INVESTIGATOR: Asim Ejaz

CONTRACTING ORGANIZATION: The University of Pittsburgh, Pittsburgh, PA

REPORT DATE: July 2022

TYPE OF REPORT: Annual

PREPARED FOR: U.S. Army Medical Research and Development Command
Fort Detrick, Maryland 21702-5012

REPORT DOCUMENTATION PAGE

Form Approved
OMB No. 0704-0188

1. REPORT DATE	2. REPORT TYPE	3. DATES COVERED
July 2022	Annual	01Jun2021-31May2022

4. TITLE AND SUBTITLE

Evaluation of Adipose-Derived Stem Cells and Metformin Combination Therapy for Radiation Fibrosis

5a. CONTRACT NUMBER
W81XWH-20-1-0327

5b. GRANT NUMBER
PR192308

5c. PROGRAM ELEMENT NUMBER

6. AUTHOR(S) Asim Ejaz

E-Mail:ejaza@upmc.edu

5d. PROJECT NUMBER
PR192308

5e. TASK NUMBER

5f. WORK UNIT NUMBER

7. PERFORMING ORGANIZATION NAME(S) AND ADDRESS(ES)

The University of Pittsburgh
3520 Fifth Ave, Pittsburgh Pennsylvania 15213-3320

8. PERFORMING ORGANIZATION REPORT NUMBER

9. SPONSORING / MONITORING AGENCY NAME(S) AND ADDRESS(ES)

U.S. Army Medical Research and Development Command
Fort Detrick, Maryland 21702-5012

10. SPONSOR/MONITOR'S ACRONYM(S)

11. SPONSOR/MONITOR'S REPORT NUMBER(S)

12. DISTRIBUTION / AVAILABILITY STATEMENT

Approved for Public Release; Distribution Unlimited

13. SUPPLEMENTARY NOTES

14. ABSTRACT

Radiation fibrosis (RF) is a long-term side effect of either therapeutic or accidental exposure to radiations. There is currently no therapy for treatment of RF. Through execution of our proposed work, we are trying to develop a therapy approach using a combination of adipose derived stem cells (ASCs) and metformin. We are testing the dose and time of the therapy and in addition testing the use of allogeneic ASCs as a mitigator for mass exposure scenarios. Data from our ongoing studies indicated that 3 million dose of ASCs showed better mitigation compared to 1 million cells. Allogeneic ASCs showed promising mitigation of RF and can be further evaluated for adaptation to countermeasure reserves. Combination of ASCs and metformin showed better mitigation compared to alone use of these agents for acute RF but is not in the significant range. Ongoing experiments will help to reach a more concrete conclusion. Mechanistic studies reveal no side effects of metformin treatment on ASCs rather metformin improves the health of ASCs by reducing oxidative stress and pro-oncogenic signaling.

15. SUBJECT TERMS
None listed.

16. SECURITY CLASSIFICATION OF:	17. LIMITATION OF ABSTRACT	18. NUMBER OF PAGES	19a. NAME OF RESPONSIBLE PERSON
			USAMRDC

a. REPORT	b. ABSTRACT	c. THIS PAGE			19b. TELEPHONE NUMBER *(include area code)*
Unclassified	Unclassified	Unclassified	Unclassified	47	

Standard Form 298 (Rev. 8-98)
Prescribed by ANSI Std. Z39.18

TABLE OF CONTENTS

1- Introduction:

Radiation fibrosis (RF) following cancer therapy or accidental radiation exposure or radiation terrorist fission bomb event causes severe functional sequelae depending on the exposed anatomical site including loss of tissue function, chronic pain and discomfort from scarring, restricted range of motion, and dysphagia. This delayed complication of radiation exposure to humans commonly damages the skin and subcutaneous muscles, as well as other internal tissues, organs, and organ systems. There are currently very limited treatment options for these symptoms, and they have low efficacy. The *long-term goal* is to develop a potent therapy for radiation fibrosis. The *overall objectives* of this proposal are to (i) evaluate the use of adipose derived stem cells (ASCs) and metformin as a combination therapy to treat radiation fibrosis and (ii) determine the molecular mechanism by which ASCs and metformin combination therapy inhibit fibrosis. The research scope comprises of two *specific aims*: 1) Determine the efficacy of ASCs and metformin combination therapy in resolution of RF. 2) Elucidate the molecular pathways by which ASCs and metformin combination therapy inhibit fibrosis: In *vitro* mechanistic studies and in *vivo* bone marrow cells migration analyses.

2- Keywords:

Radiations, cancer, fibrosis, adipose stem cells, cell therapy, metformin, adult stem cells

3- Accomplishments:

3.1- Major goals of the project

Following are the major goals stated in the approved SOW.
1: Determine the dose and timings of syngeneic ASCs and metformin combination therapy for radiation fibrosis.
2: Determine the dose and timings of allogeneic ASCs and metformin combination therapy for radiation fibrosis.
3: Mechanistic studies
4: Data analyses, manuscript for publication, and future grant proposal preparation

3.2- Accomplishment

3.2.1- Regulatory approval of IACUC, ACURO, and HRPO

During this funding period, our team accomplished successful approval of the IACUC protocol from the University of Pittsburgh which was presented to ACURO and was approved. In addition, we also obtained the Institutional IRB approval for use of human tissue-derived cells and got the approval from HRPO.

3.2.2: Determine the dose and timings of syngeneic adipose-derived stem cells (ASCs) and metformin combination therapy for radiation fibrosis

In the previous reporting year, we showed the results of experiments conducted to optimize the dose of the adipose-derived stem cells for the mitigation of radiation-induced fibrosis. Based on those results we selected a dose of $3x10^6$ ASCs for therapeutical application in mice.

Experiment 1:
To study the combined effect of ASCs and metformin combination therapy, we tested a dose of $3x10^6$ ASCs alone, metformin alone, or a combination of $3x10^6$ ASCs or metformin starting at day 1 post 40 Gy irradiation. Our experimental groups were:
1- Irradiated-control PBS injection
2- Irradiated-$3x10^6$ syngeneic ASCs injection
3- Irradiated-Metformin alone injection
4- Irradiated-$3x10^6$ syngeneic ASCs + Metformin injection

ASCs were injected subcutaneously at the irradiation site 1-day post-irradiation and metformin was given intraperitoneal 3 times a week until sacrifice at day 42 post-irradiation. Analyses included visual observation and recording of the wound healing and skin texture improvement, functional analysis by measurement of limb excursion motion, and histological analyses of irradiated skin tissue using H&E and Masson's Trichrome staining. The thickness of the skin epithelium was measured and plotted. The histological sections of the skin were graded for inflammation score, fibrosis score, vascular score, and cellular alterations score following the published guidelines.[1]

Results:

We observed and imaged the progression of irradiation-induced fibrotic wound starting day 21 post-irradiation. Most of the mice in the irradiated control group developed fibrotic wounds reflected by skin constriction and hair loss (Fig 1A, supplementary 1A). Injection of ASCs (Fig 1B, supplementary 1B), metformin (1C, supplementary 1C), or a combination of both ASCs and metformin (1D, supplementary 1D) resulted in improvement in skin architecture and heeling of fibrotic wounds.

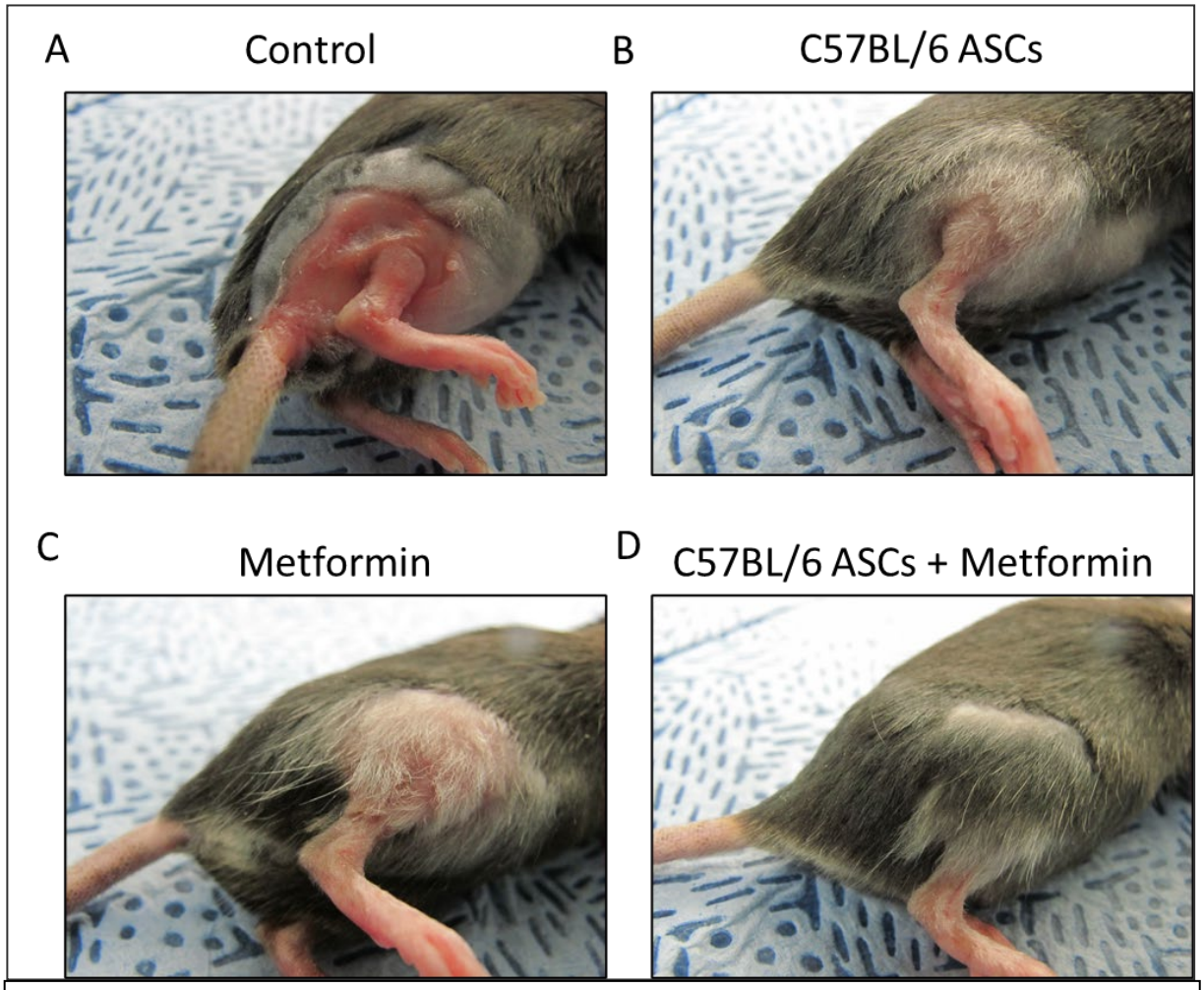

Figure 1: Mice were 40Gy irradiated followed by injection of PBS control (A), C57BL/6 ASCs (B), Metformin (C), or C57BL/6+Metformin at day 1 post-irradiation.


Supplementary 1A
Irradiated Control
Mice 1
Mice 2
Mice 3
Mice 4
Mice 5
Mice 6
day21
day28
day35
day42
Mice 7
Mice 8
Mice 9
Mice 10
Mice 11
Mice 12
day21
day28
day35
day42

Supplementary 1B

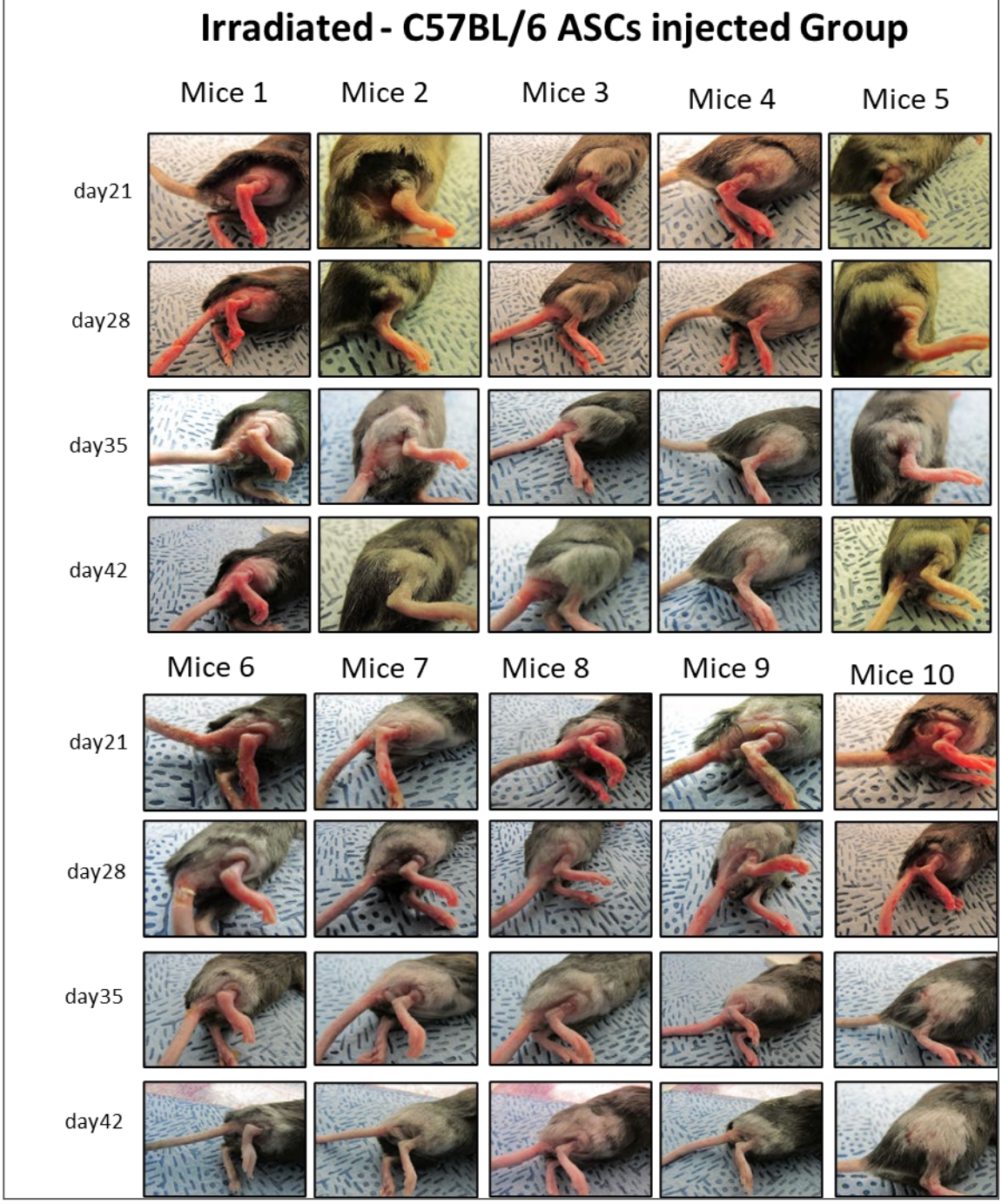

Supplementary 1C

Supplementary 1D

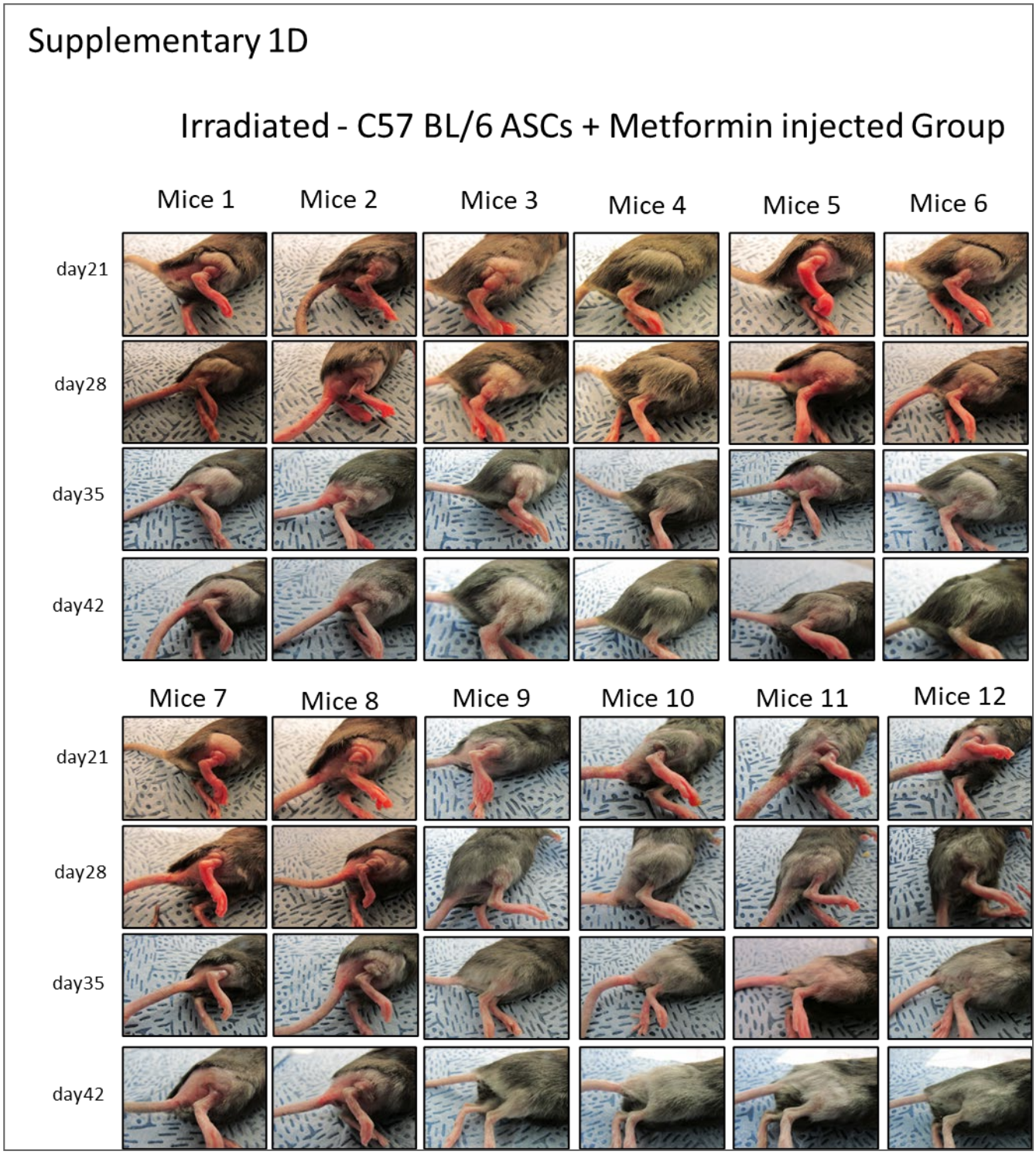

Measuring the degree of limb excursion as a functional assay of fibrosis development, we observed that 40 Gy irradiation exposure resulted in a significant decrease in the limb excursion ability in control mice by days 35 and 42 post-irradiation (Figure 2). A single injection of autologous ASCs on day 1 post-irradiation or metformin injection 3 times weekly starting at day 1 post-irradiation resulted in a significant recovery of the irradiated limb movement by day 42 post-irradiation. Combination therapy of autologous ASCs injected on day 1 post-irradiation and metformin 3 times weekly starting day 1 post-irradiation showed improved recovery in limb excursion as compared to the single treatment regime but the extent of the improvement was not significant (Figure 2).

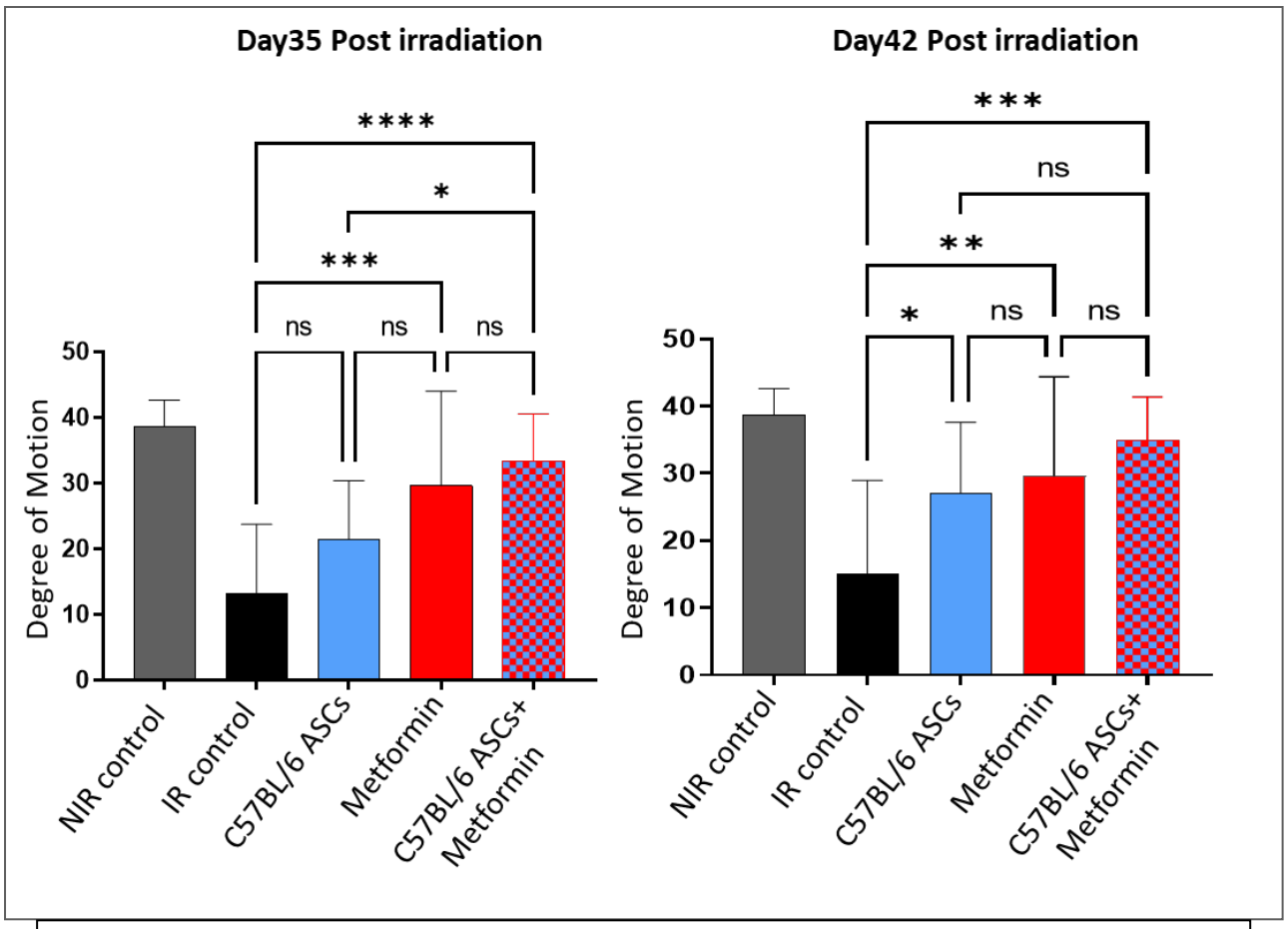

Figure 2: Mice were 40Gy irradiated followed by injection of PBS control (A), C57BL/6 ASCs (B), Metformin (C), or C57BL/6+Metformin at day 1 post-irradiation. Excursion of the limb was measured on day 35 and day 42 post-irradiation. $p<0.05$=*, $p<0.005$=**, $p<0.0005$=***, $p<0.00005$=****, ns=non-significant.

Masson's Trichrome staining of the irradiated skin sections harvested on day 42 post-irradiation revealed, thickened epithelium, hyperplastic epidermis having deep rete pegs, and the presence of parakeratotic crusts on the epithelium surface and deposition of excessive extracellular matrix. Treatment with autologous ASCs, metformin, or a combination of ASCs and metformin resulted in the preservation of epithelium and epidermis structure (Figure 3, Supplementary Figure 2).

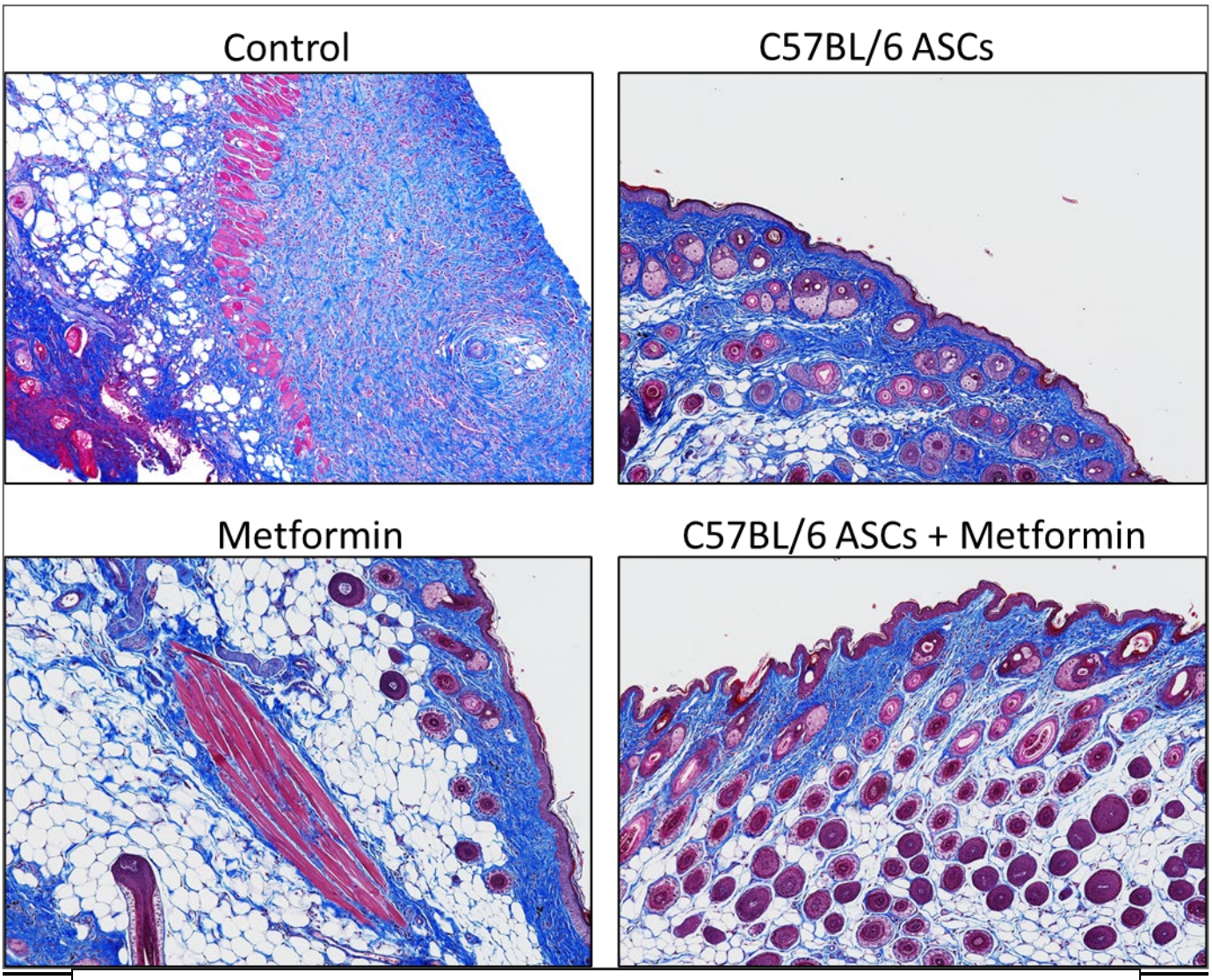

Figure 3: Irradiated skin was harvested on day 42 post-irradiation and fixed. Paraffin blocks of fixed tissues were prepared and sectioned. Masson's Trichrome staining of the skin sections was performed.

Supplementary Figure 2

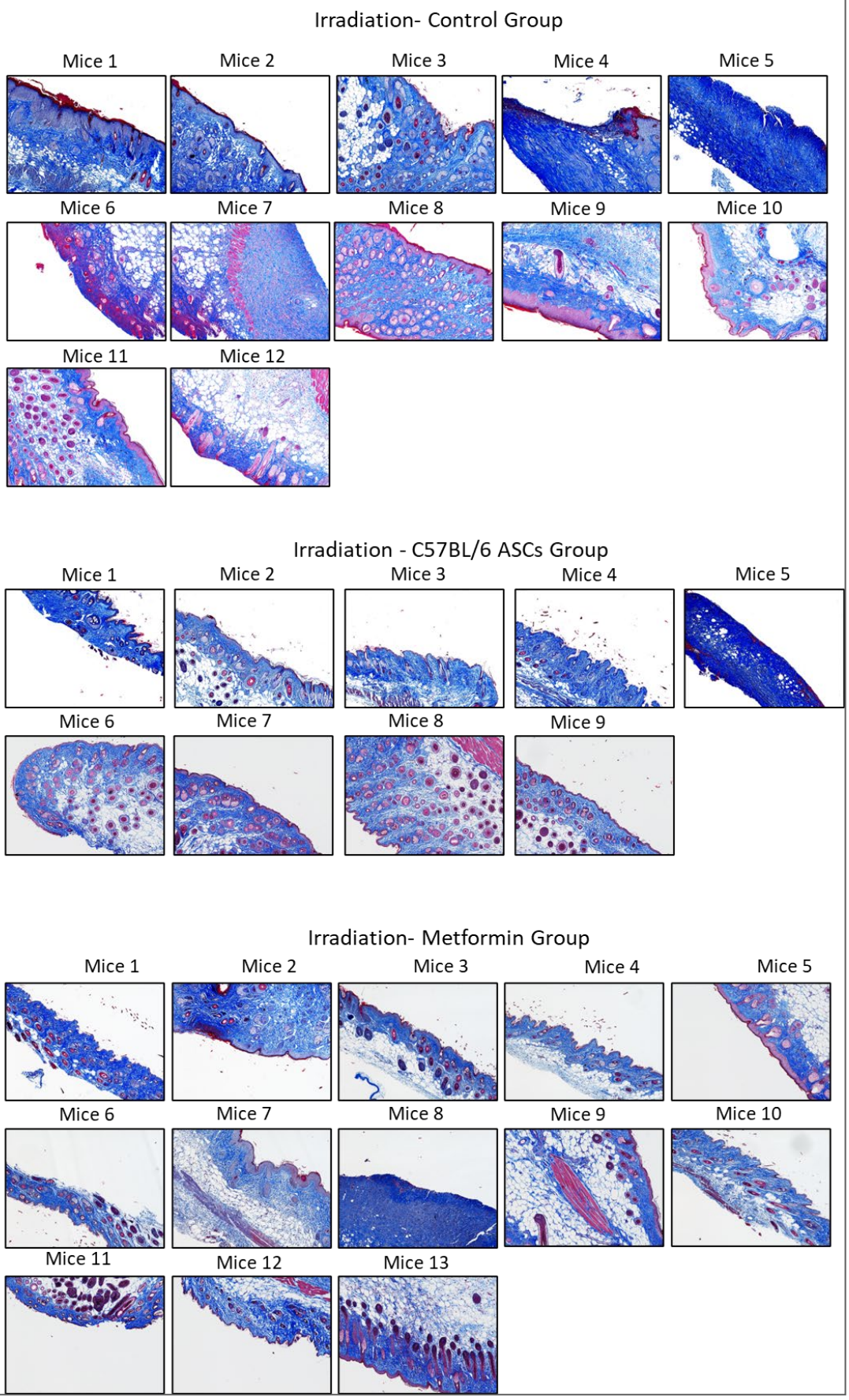

Supplementary Figure 2

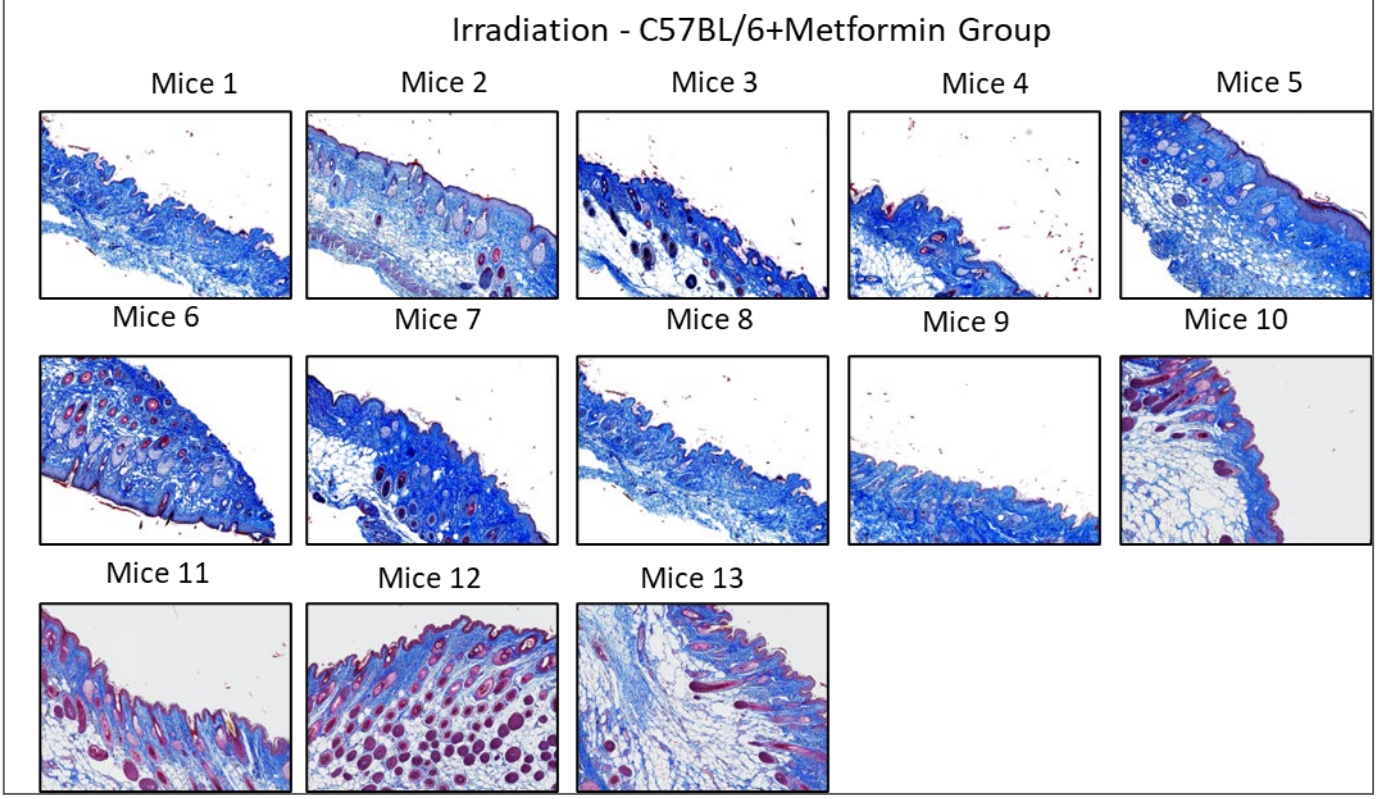

Evaluation of the skin section for inflammation score, fibrosis score, vascular score, and cellular alteration score was performed following the published scoring criteria.[1] Results revealed that both single therapy regimes or a combination resulted in a significant improvement in the scores (Figure 4).

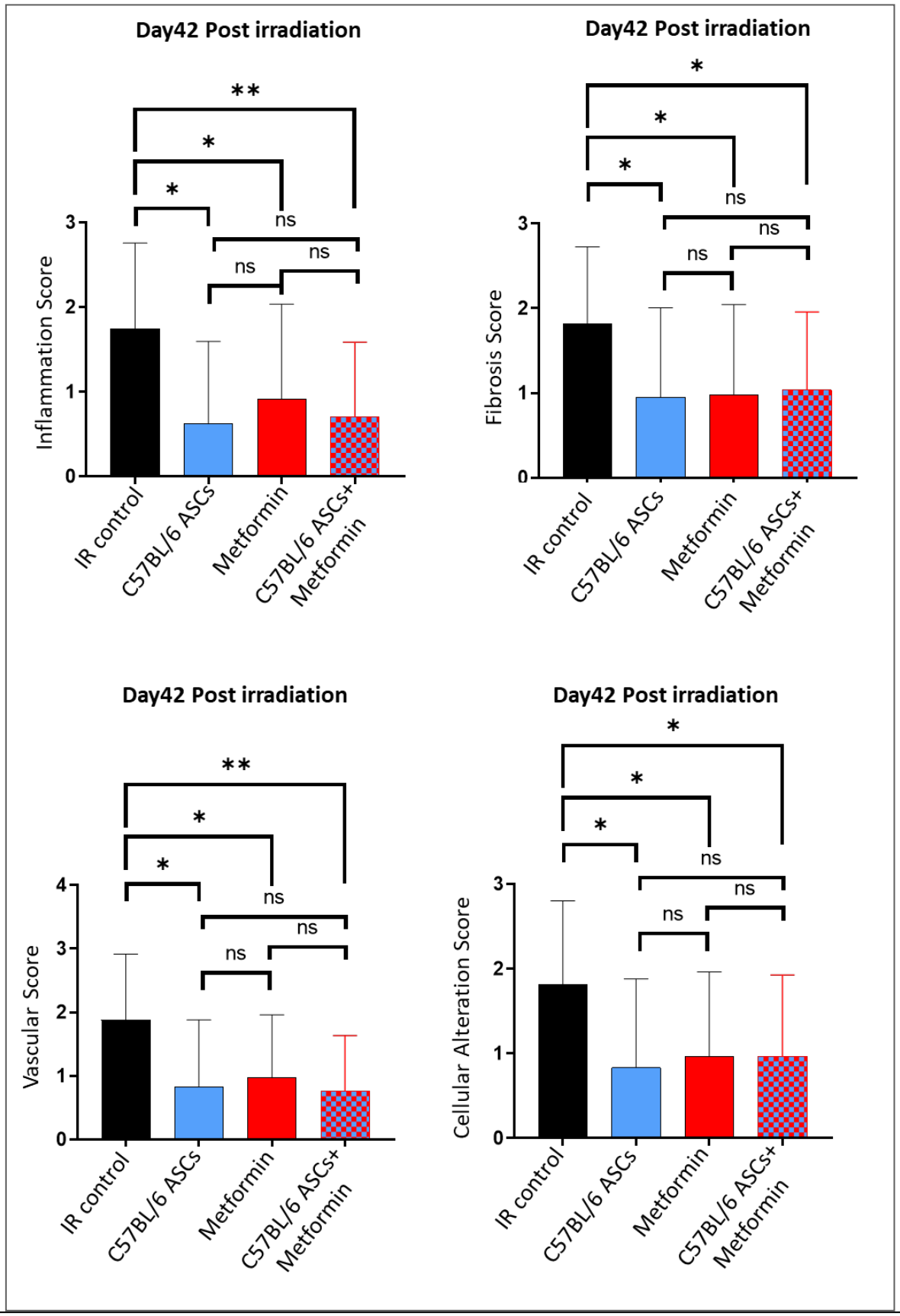

Figure 4: Irradiated skin was harvested on day 42 post-irradiation and fixed. Paraffin blocks of fixed tissues were prepared and sectioned. Masson's Trichrome staining of the skin sections was performed and scored for the abovementioned criteria. $p<0.05$=*, $p<0.005$=**, and ns=non-significant.

Experiment 2:

Through experiment 1 we studied the effect of combination therapy immediately after irradiation exposure when no fibrosis is developed. To study the combined effect of ASCs and metformin combination therapy at late time points after exposure we selected day 14 as the therapy time point. Our previous studies showed that by day 14 post-irradiation we observed signs of fibrosis progression supported by the reduction in limb excursion and up-regulation of molecular signatures of fibrosis.[2] We tested a dose of $3x10^6$ ASCs alone, metformin alone, or a combination of $3x10^6$ ASCs or metformin starting at day 14 post 40 Gy irradiation. Our experimental groups were:

1- Irradiated-control PBS injection
2- Irradiated-$3x10^6$ syngeneic ASCs injection
3- Irradiated-Metformin alone injection
4- Irradiated-$3x10^6$ syngeneic ASCs + Metformin injection

ASCs were injected subcutaneously at the irradiation site 14-day post-irradiation and metformin was given intraperitoneal 3 times a week until sacrifice at day 42 post-irradiation. Analyses included visual observation and recording of the wound healing and skin texture improvement, functional analysis by measurement of limb excursion motion, and histological analyses of irradiated skin tissue using H&E and Masson's Trichrome staining. The thickness of the skin epithelium was measured and plotted. The histological sections of the skin were graded for inflammation score, fibrosis score, vascular score, and cellular alterations score following the published guidelines.[1]

Results:

We observed and imaged the progression of irradiation-induced fibrotic wound starting day 21 post-irradiation. Most of the mice in the irradiated control group developed fibrotic wounds reflected by skin constriction and hair loss (Fig 5A, supplementary 3A). Injection of ASCs (Fig 5B, supplementary 3B), metformin (5C, supplementary 3C), or a combination of both ASCs and metformin (5D, supplementary 3D) resulted in improvement in skin architecture and heeling of fibrotic wounds.

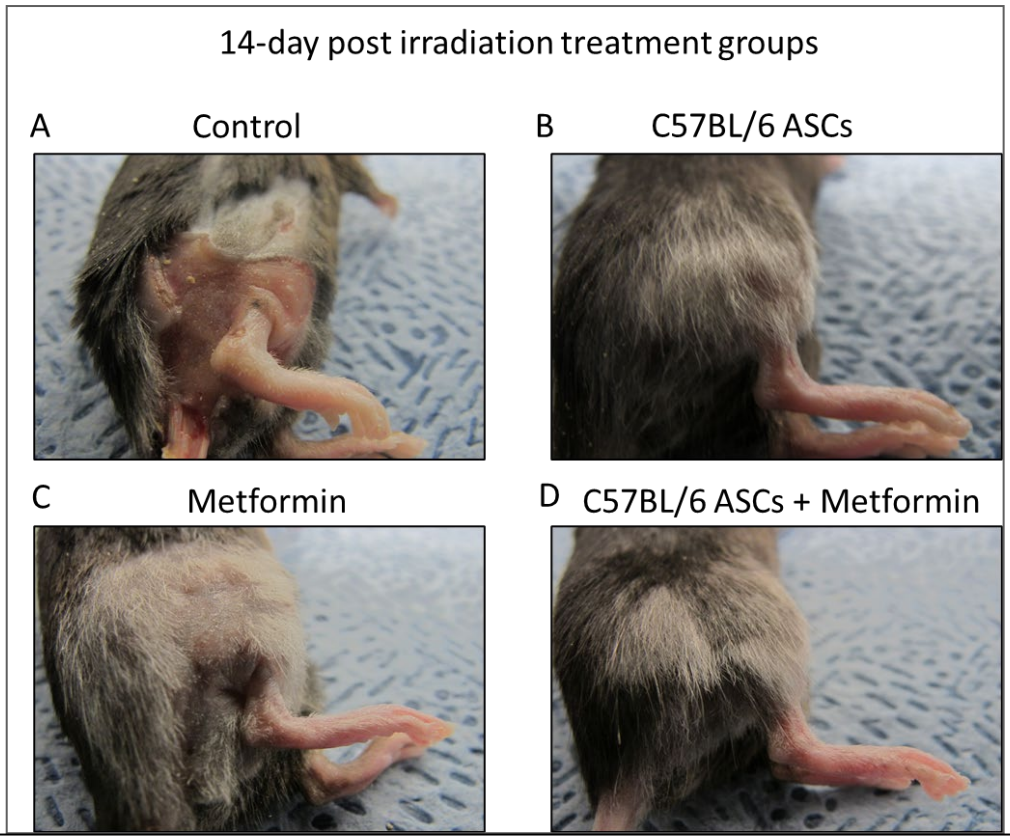

Figure 5: Mice were 40Gy irradiated followed by injection of PBS control (A), C57BL/6 ASCs (B), Metformin (C), or C57BL/6+Metformin at day 14 post-irradiation.

Supplementary 3A

Control

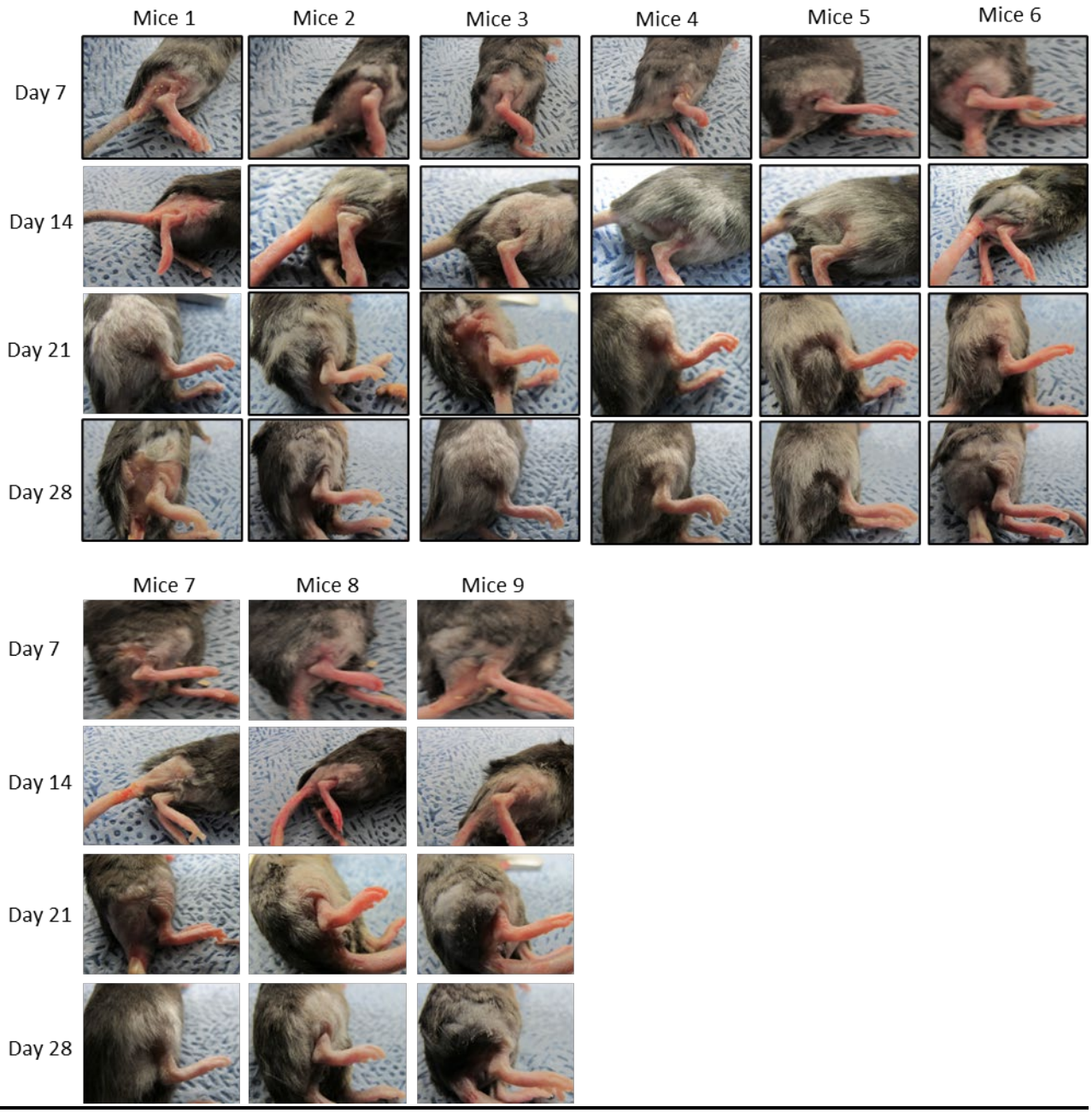

Supplementary 3B **C57BL/6 ASCs**

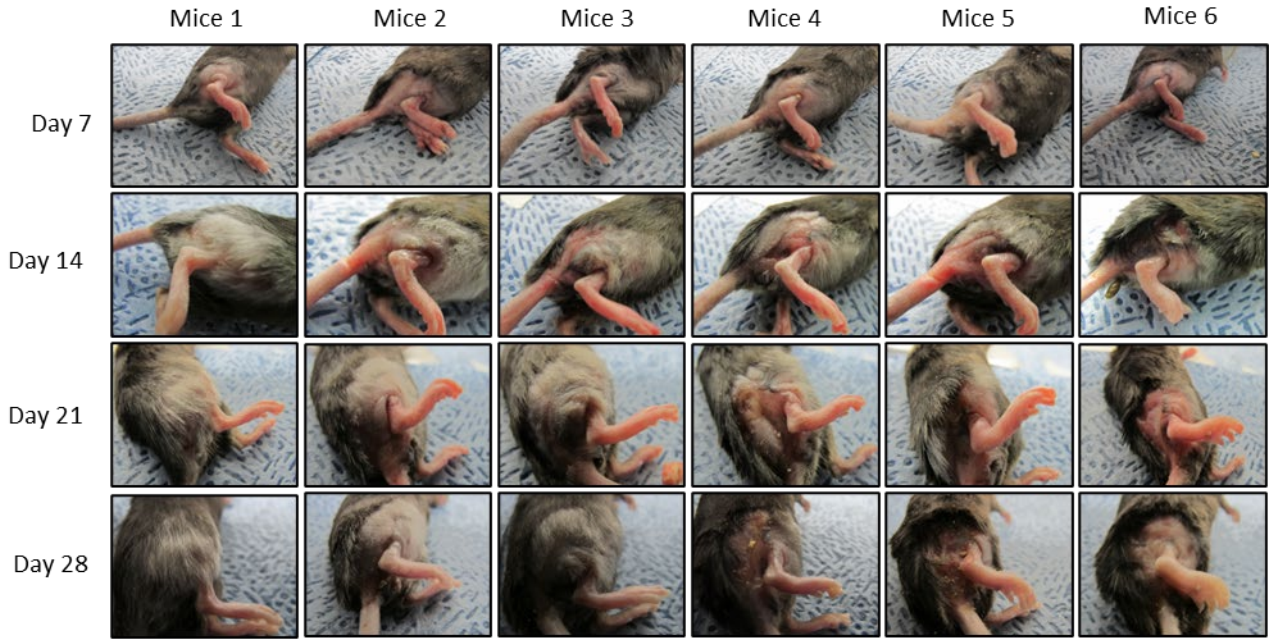

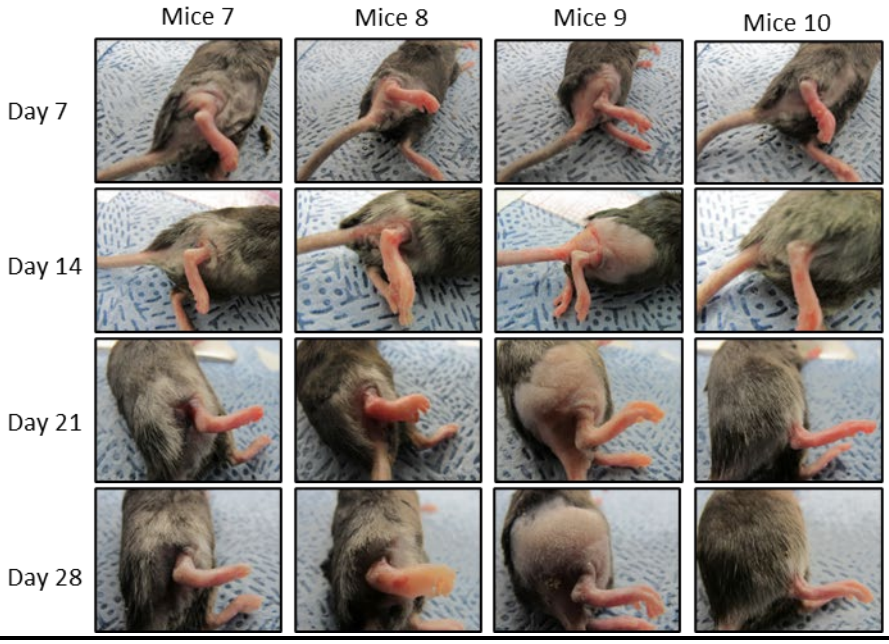

Supplementary 3C

Metformin

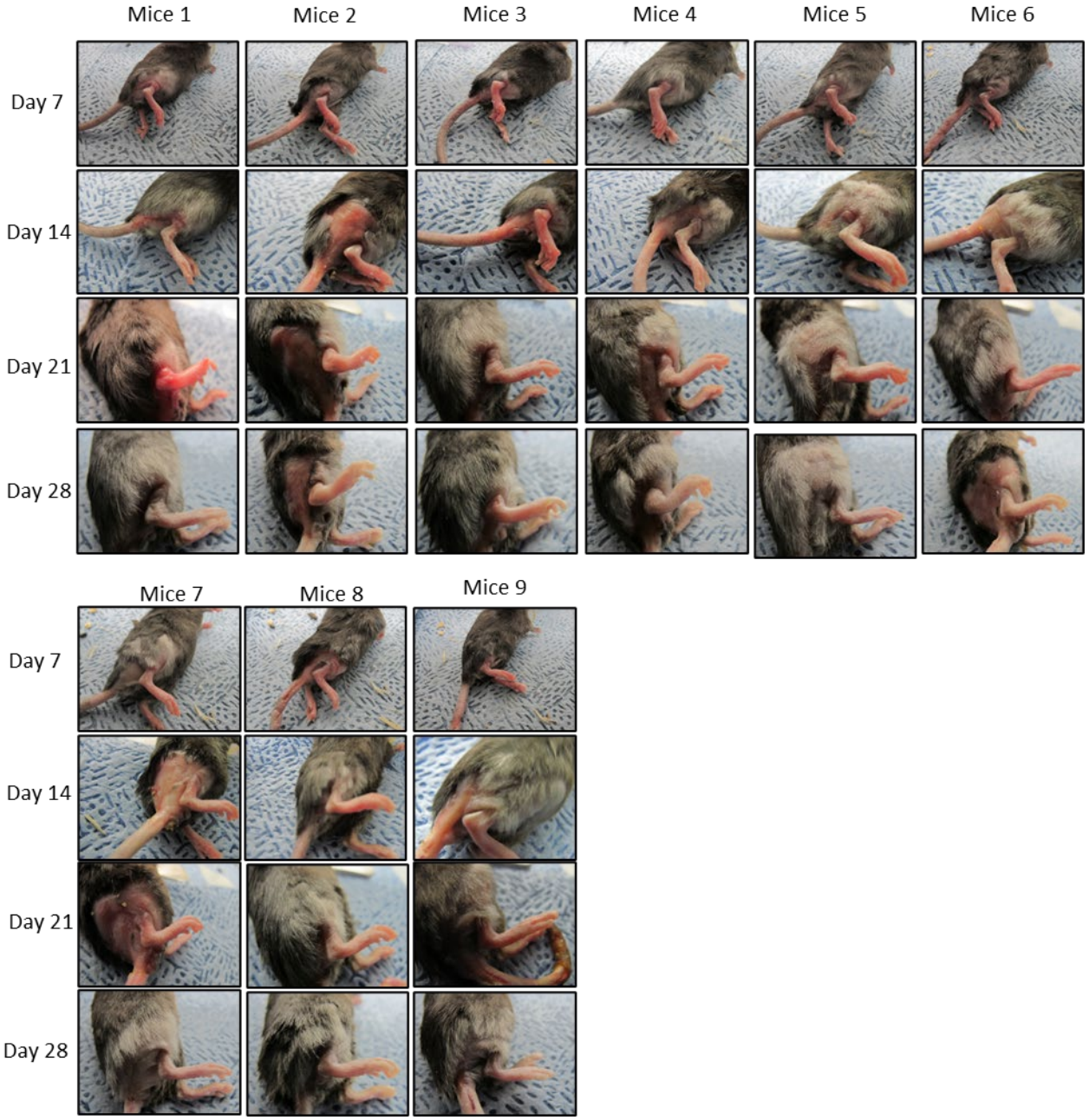

Supplementary 3D

C57BL/6 ASCs +Metformin

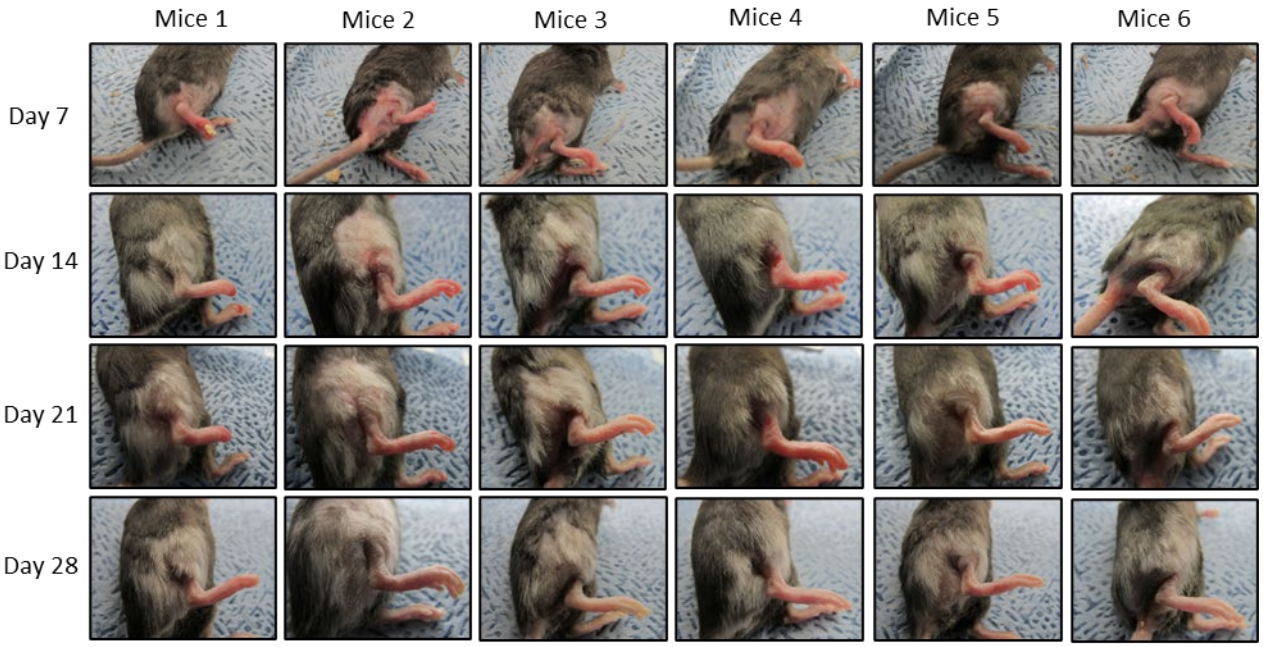

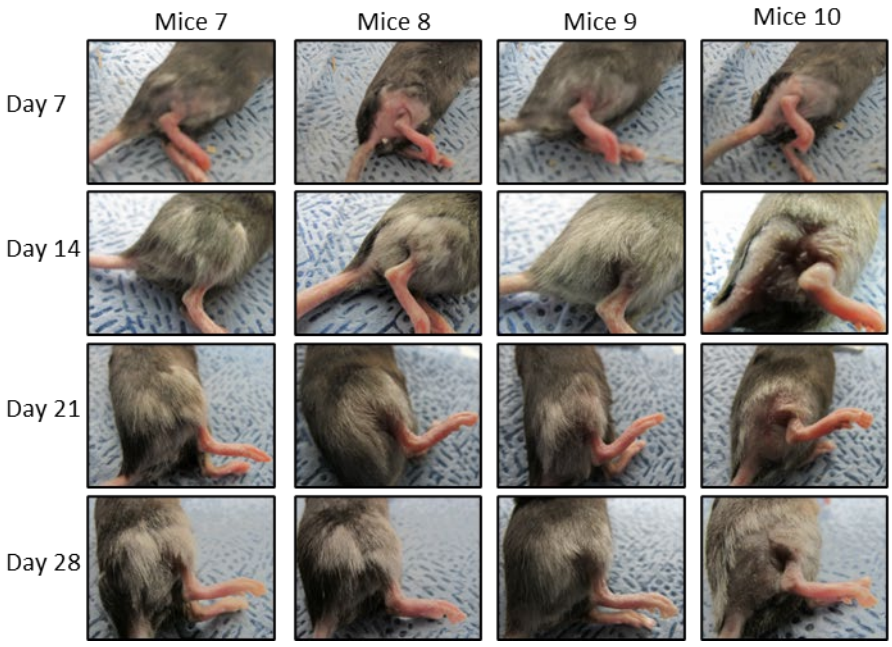

Measuring the degree of limb excursion as a functional assay of fibrosis development, we observed that 40 Gy irradiation exposure resulted in a significant decrease in the limb excursion ability in control mice by days 35 and 42 post-irradiation (Figure 6). A single injection of autologous ASCs on day 14 post-irradiation resulted in a significant recovery of the irradiated limb movement by day 42 post-irradiation. Interestingly, although metformin-only injection resulted in improvement of limb excursion the magnitude of the recovery was not significant (Figure 6). We observed a significant improvement in limb excursion upon treatment with a combination of autologous ASCs and metformin therapy compared to control, ASCs alone, or metformin alone. (Figure 6).

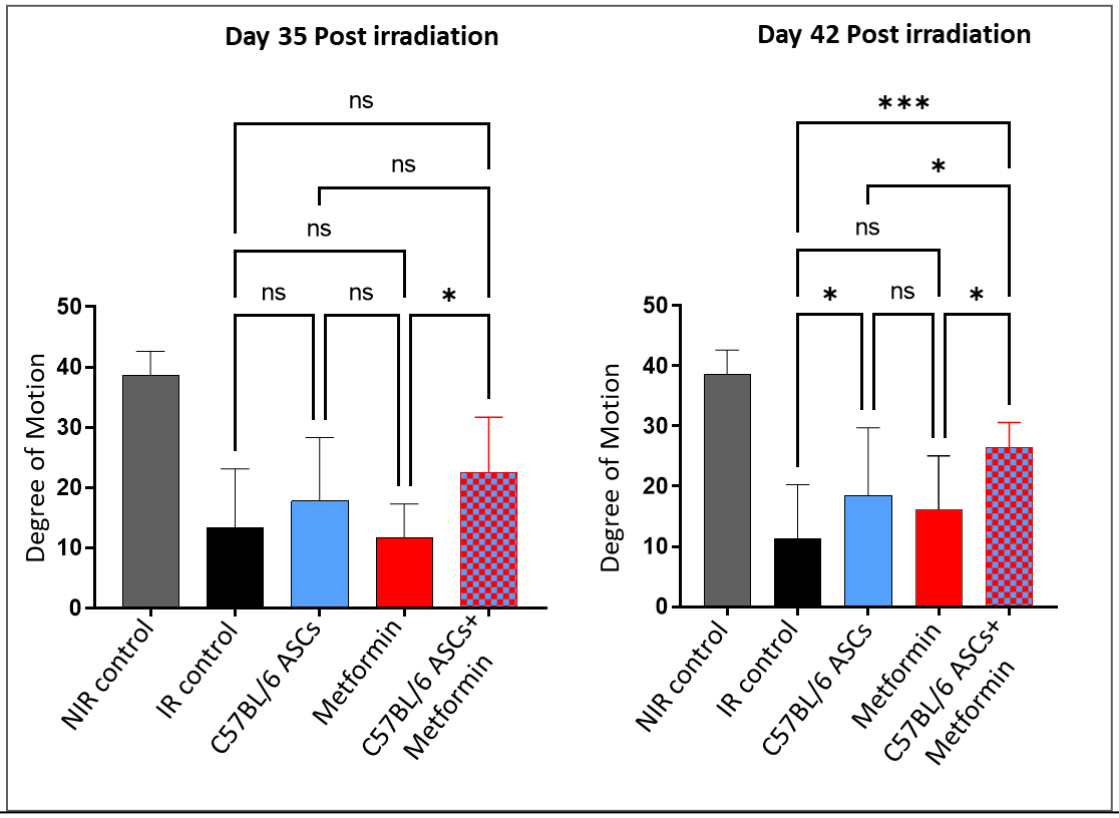

Figure 6: Mice were 40Gy irradiated followed by injection of PBS control (A), C57BL/6 ASCs (B), Metformin (C), or C57BL/6+Metformin at day 14 post-irradiation. Excursion of the limb was measured on day 35 and day 42 post-irradiation. $p<0.05$=*, $p<0.005$=***, and ns=non-significant.

Conclusion: We conclude that both autologous ASCs and metformin showed mitigation of radiation fibrosis. At the very early stage post-exposure when fibrosis has not developed metformin showed a higher mitigation efficiency and the combination therapy of ASCs and metformin showed a non-significant improvement compared to both agents used alone.
While at the later time points post-radiation exposure when the fibrosis has progressed metformin showed a relatively weak mitigation effect compared to autologous ASCs. A combination of both showed the best mitigation of fibrosis.
Based on these results we hypothesize that mechanistically metformin blocks the development of fibrosis but has relatively lesser regeneration capability to reverse the already established fibrotic wound. On the other hand, autologous ASCs compensate and provide the regeneration property.

Work in progress:
We are currently performing the gene expression analysis of the skin samples from all the above-mentioned experimental conditions and groups.

3.2.3: Determine the dose and timings of allogeneic ASCs and metformin combination therapy for radiation fibrosis.

In the previous reporting year, we showed the results of experiments conducted to optimize the dose of the adipose-derived stem cells for the mitigation of radiation-induced fibrosis. Based on those results we selected a dose of $3x10^6$ ASCs for therapeutical application in mice.

Experiment 3:

To study the combined effect of allogeneic ASCs (ASCs isolated from FVB mice injected in C57BL/6 host) and metformin combination therapy, we tested a dose of $3x10^6$ ASCs alone, metformin alone, or a combination of $3x10^6$ ASCs or metformin starting at day 1 post 40 Gy irradiation. Our experimental groups were:

1- Irradiated-control PBS injection
2- Irradiated-$3x10^6$ allogeneic ASCs injection
3- Irradiated-Metformin alone injection
4- Irradiated-$3x10^6$ allogeneic ASCs + Metformin injection

ASCs were injected subcutaneously at the irradiation site 1-day post-irradiation and metformin was given intraperitoneal 3 times a week until sacrifice at day 42 post-irradiation. Analyses included visual observation and recording of the wound healing and skin texture improvement, functional analysis by measurement of limb excursion motion, and histological analyses of irradiated skin tissue using H&E and Masson's Trichrome staining. The thickness of the skin epithelium was measured and plotted. The histological sections of the skin were graded for inflammation score, fibrosis score, vascular score, and cellular alterations score following the published guidelines.[1]

Results:

We observed and imaged the progression of irradiation-induced fibrotic wound starting day 21 post-irradiation. Most of the mice in the irradiated control group developed fibrotic wounds reflected by skin constriction and hair loss (Fig 7A, supplementary 4A). Injection of ASCs (Fig 7B, supplementary 4B), metformin (7C, supplementary 4C), or a combination of both ASCs and metformin (7D, supplementary 4D) resulted in improvement in skin architecture and heeling of fibrotic wounds.

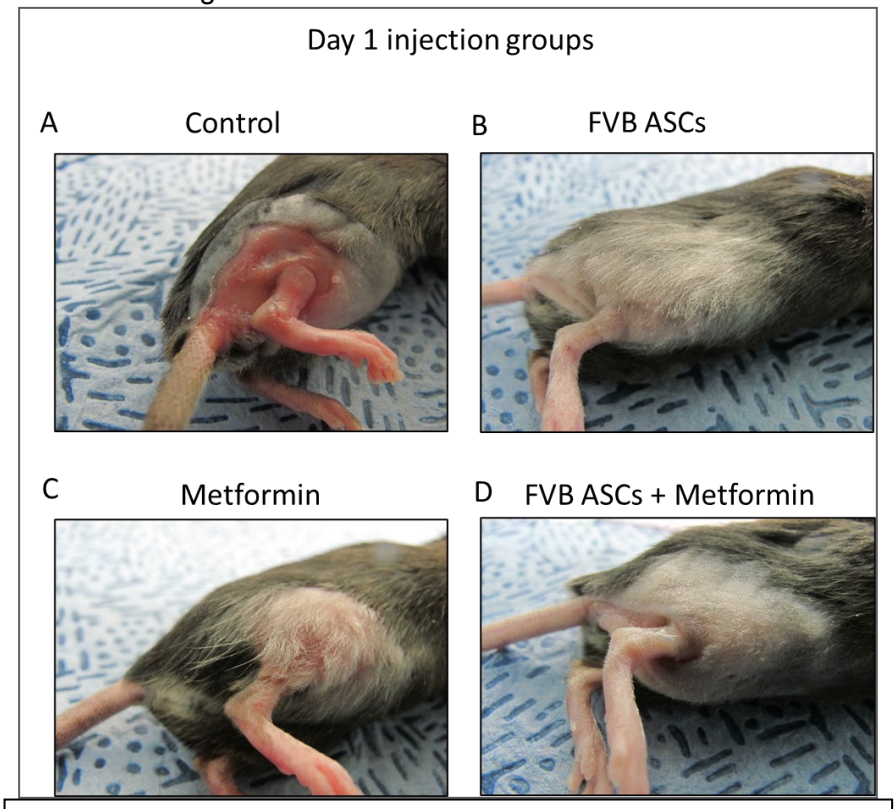

Figure 7: Mice were 40Gy irradiated followed by injection of PBS control (A), FVB ASCs (B), Metformin (C), or FVB+Metformin at day 1 post-irradiation.

Supplementary 4A **Irradiated Control**

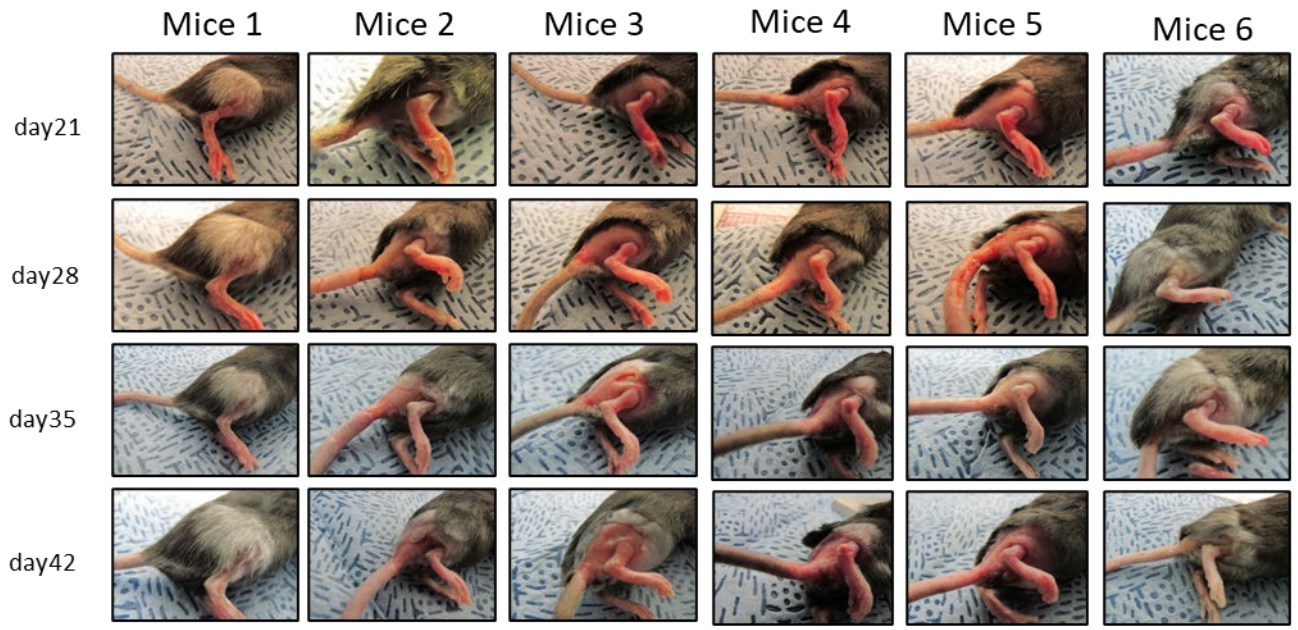

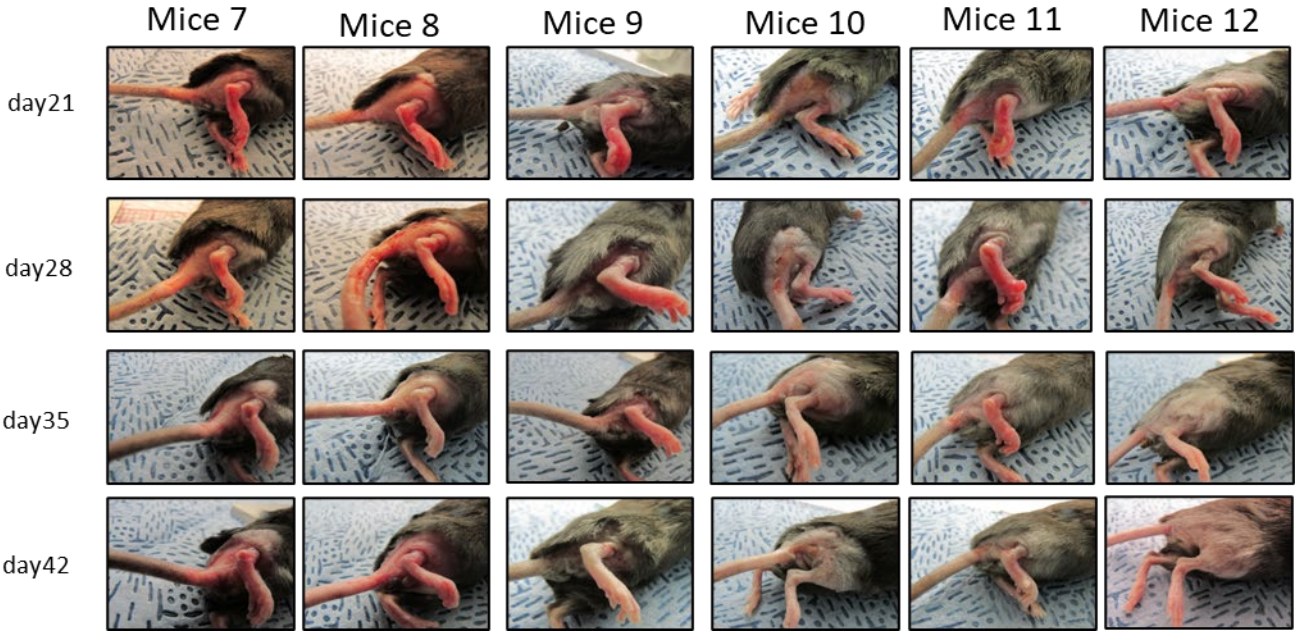

Supplementary 4B **Irradiated- FVB ASCs injected Group**

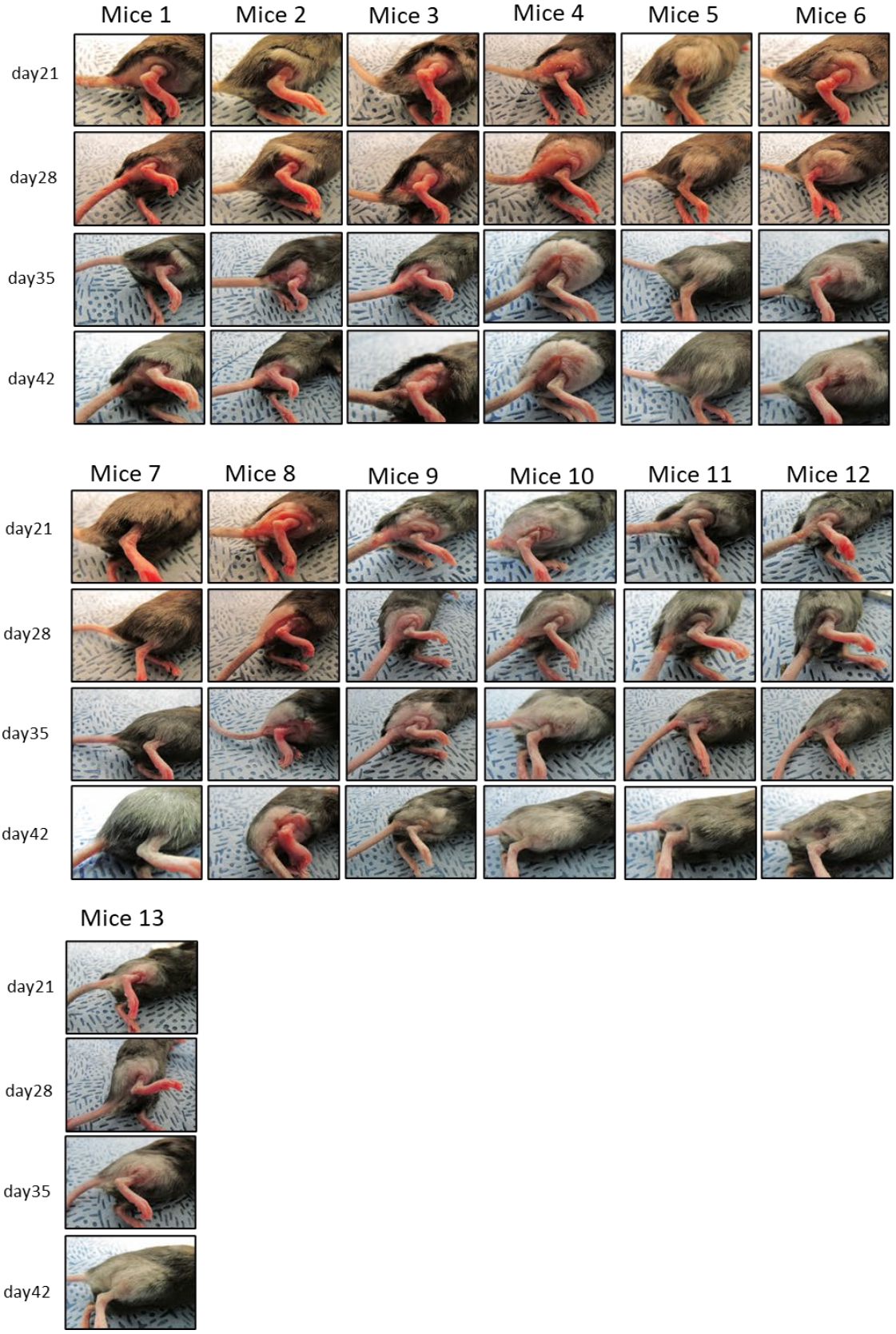

Supplementary 4C

Irradiated - Metformin injected Group

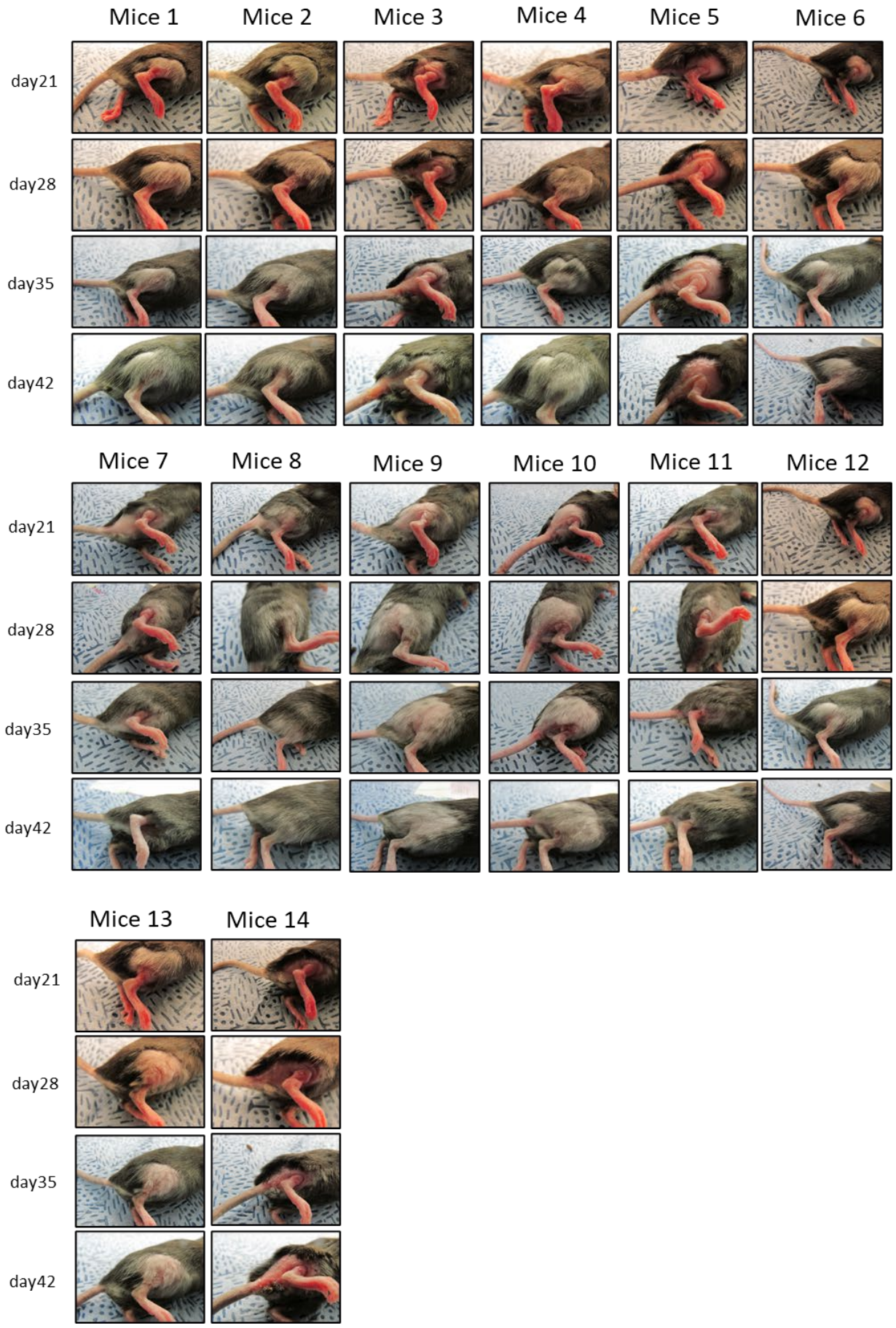

Supplementary 4D

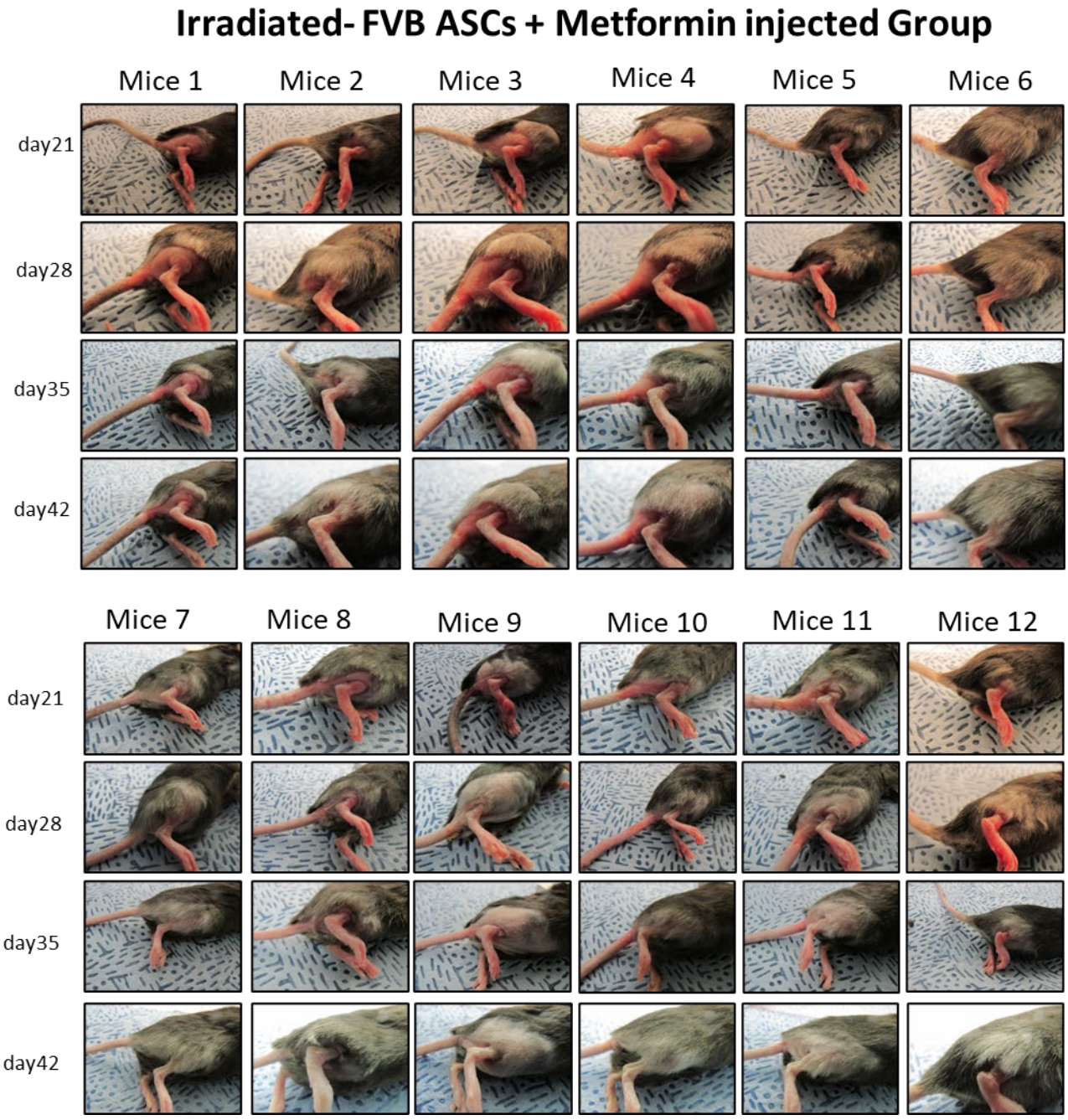

Measuring the degree of limb excursion as a functional assay of fibrosis development, we observed that 40 Gy irradiation exposure resulted in a significant decrease in the limb excursion ability in control mice by days 35 and 42 post-irradiation (Figure 8). A single injection of allogeneic ASCs on day 1 post-irradiation or metformin injection 3 times weekly starting at day 1 post-irradiation resulted in a significant recovery of the irradiated limb movement by day 42 post-irradiation. No synergism in mitigation improvement was observed by the combination therapy of allogeneic ASCs injected on day 1 post-irradiation and metformin 3 times weekly starting day 1 post-irradiation (Figure 8).

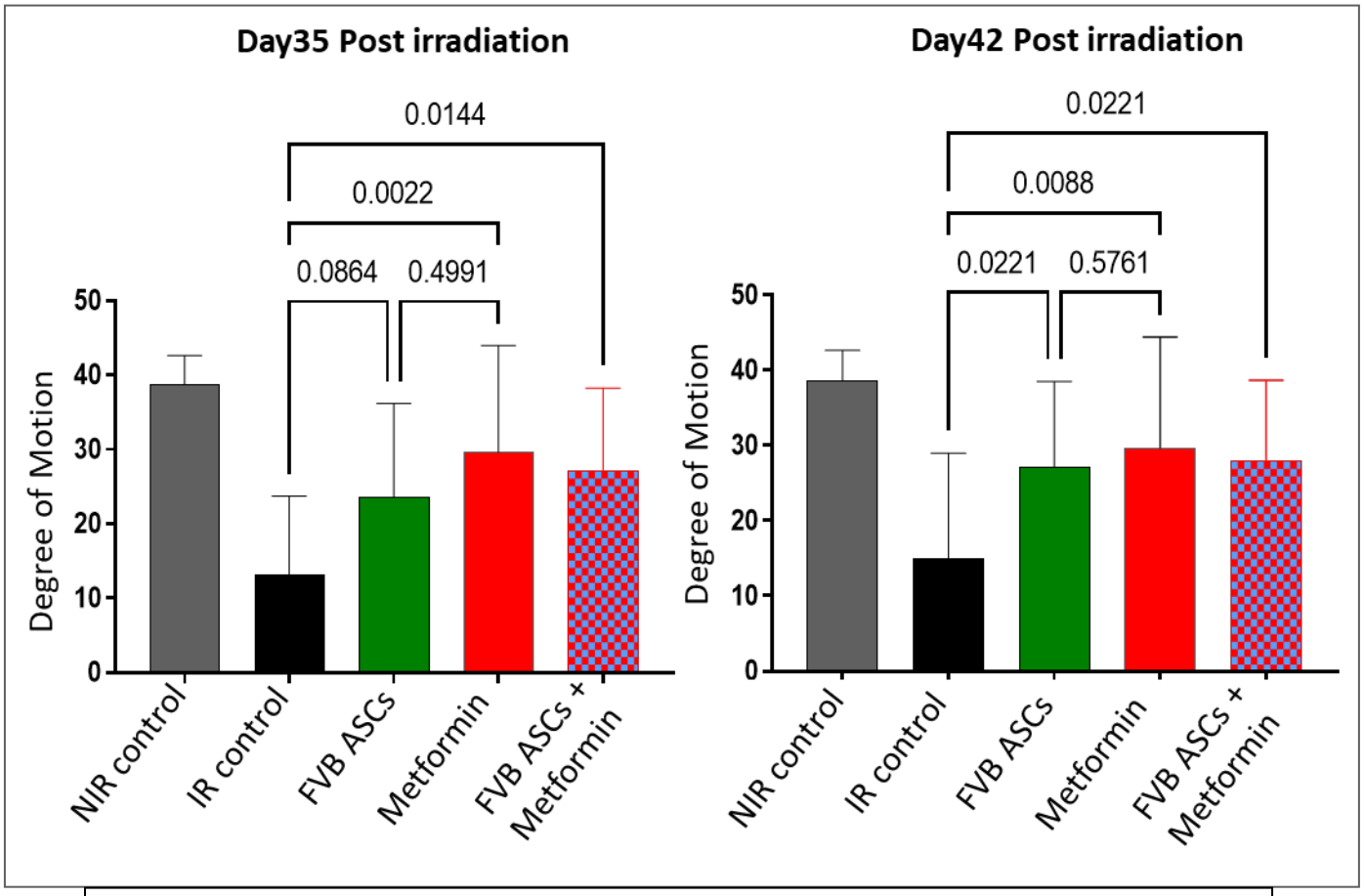

Figure 8: Mice were 40Gy irradiated followed by injection of PBS control (A), FVB ASCs (B), Metformin (C), or FVB ASCs+Metformin at day 1 post-irradiation. Excursion of the limb was measured on day 35 and day 42 post-irradiation.

Masson's Trichrome staining of the irradiated skin sections harvested on day 42 post-irradiation revealed, thickened epithelium, hyperplastic epidermis having deep rete pegs, and the presence of parakeratotic crusts on the epithelium surface and deposition of excessive extracellular matrix. Treatment with allogeneic ASCs, metformin, or a combination of allogeneic ASCs and metformin resulted in the preservation of epithelium and epidermis structure (Figure 9, Supplementary Figure 5).

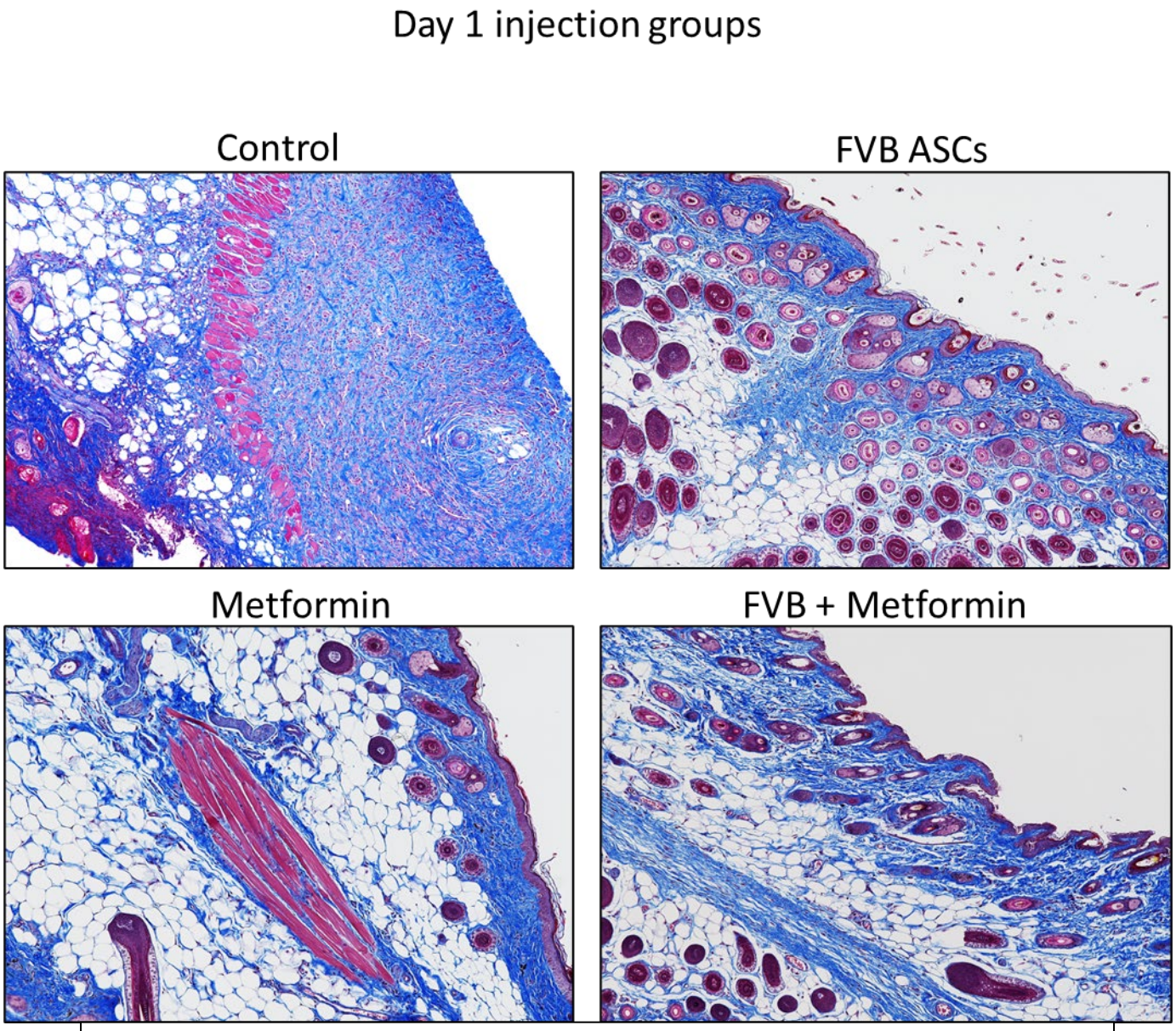

Figure 9: Irradiated skin was harvested on day 42 post-irradiation and fixed. Paraffin blocks of fixed tissues were prepared and sectioned. Masson's Trichrome staining of the skin sections was performed.

Supplementary Fig 5

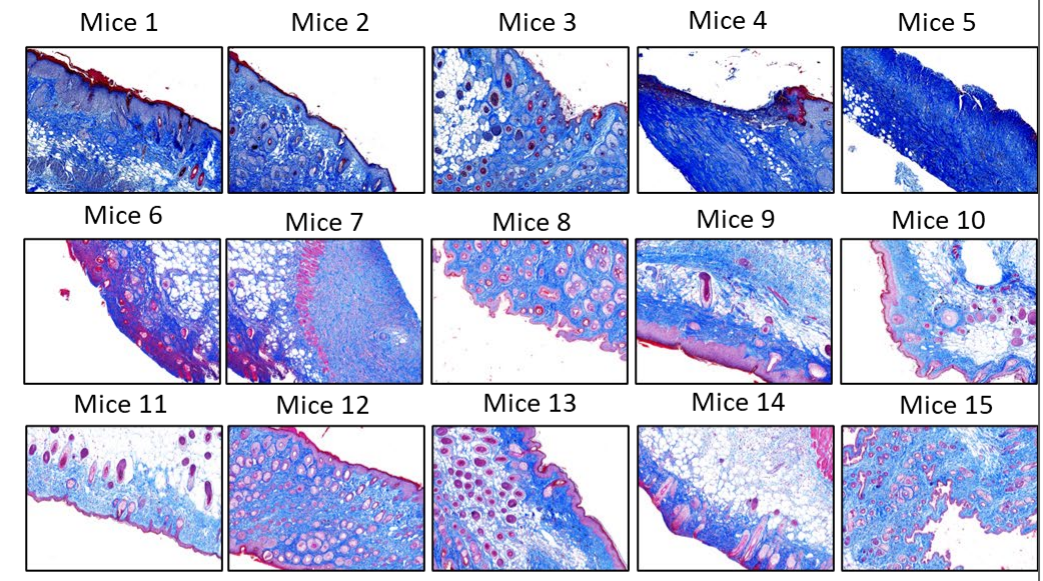

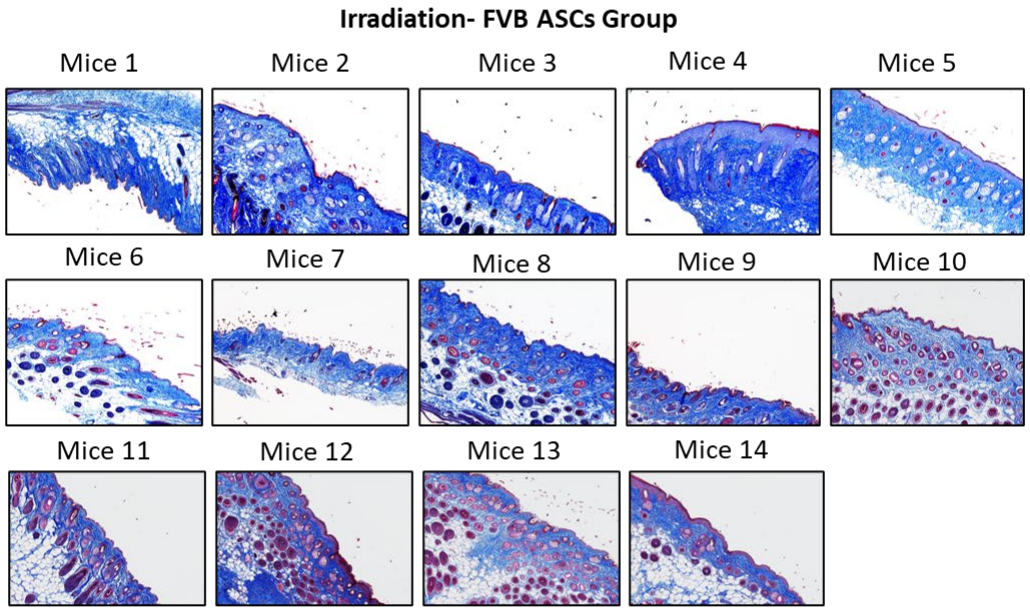

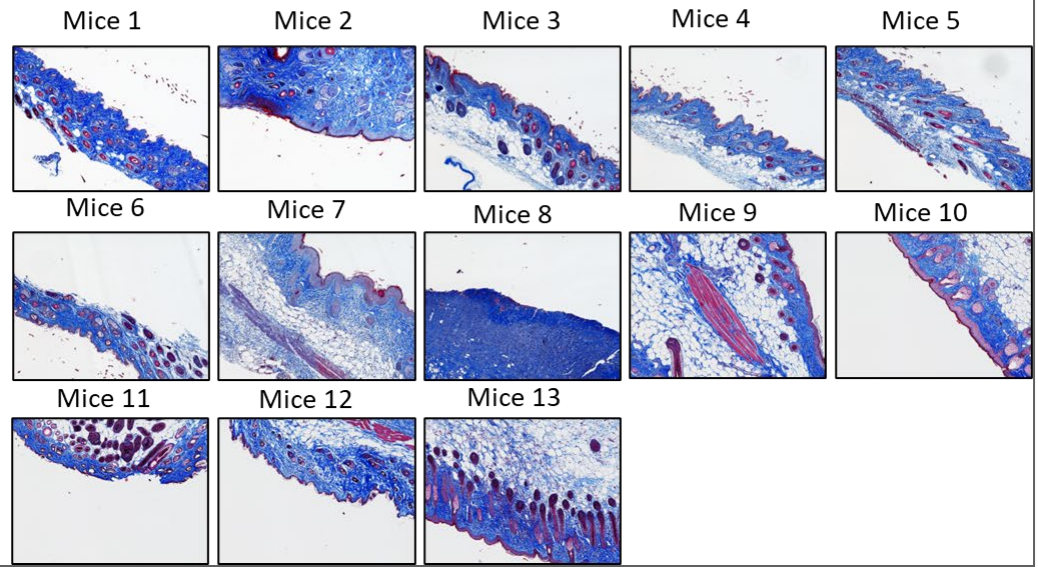

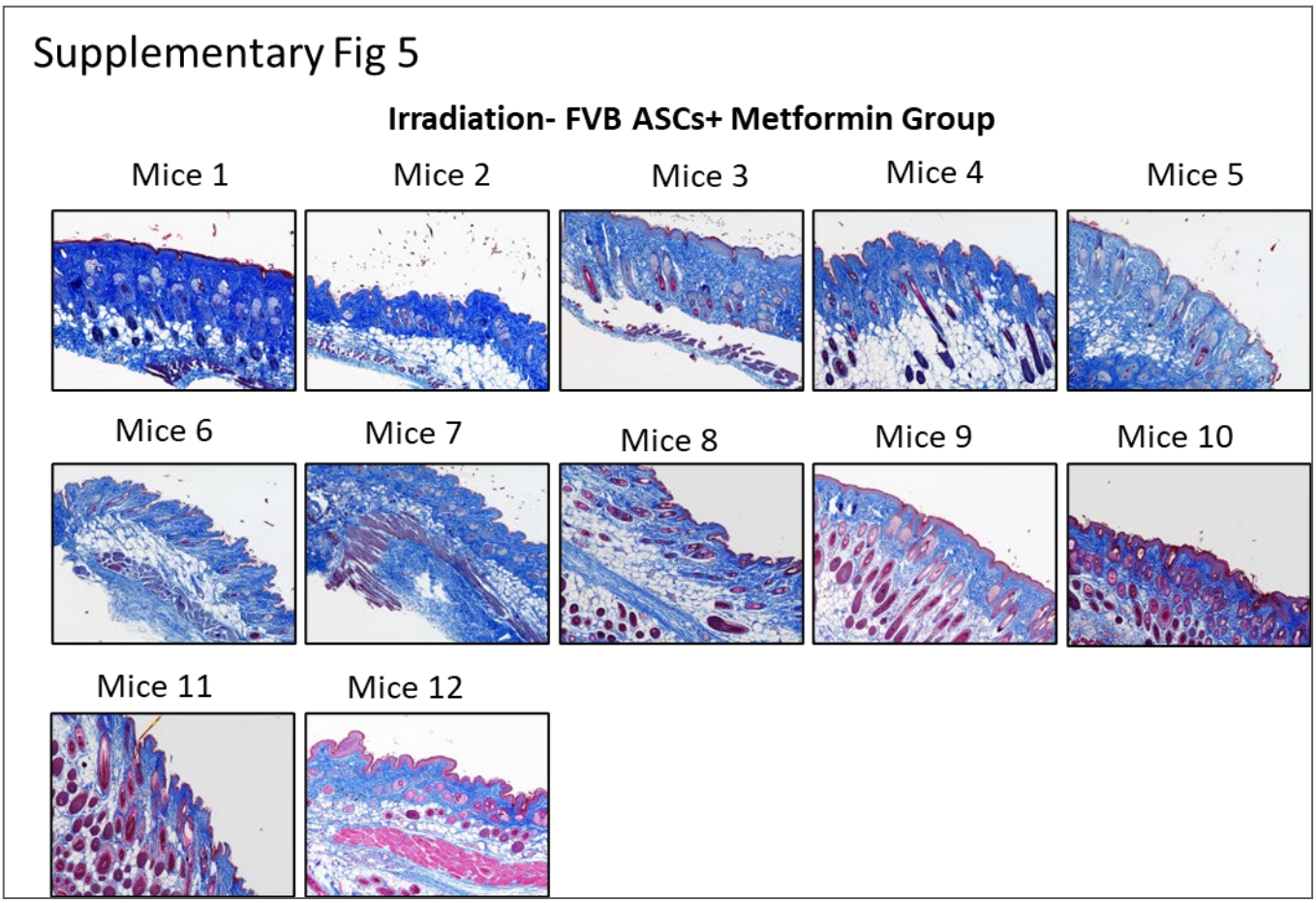

Evaluation of the skin section for inflammation score, fibrosis score, vascular score, and cellular alteration score was performed following the published scoring criteria.[1] Results revealed that both single therapy regimes or a combination resulted in a significant improvement in the scores (Figure 10).

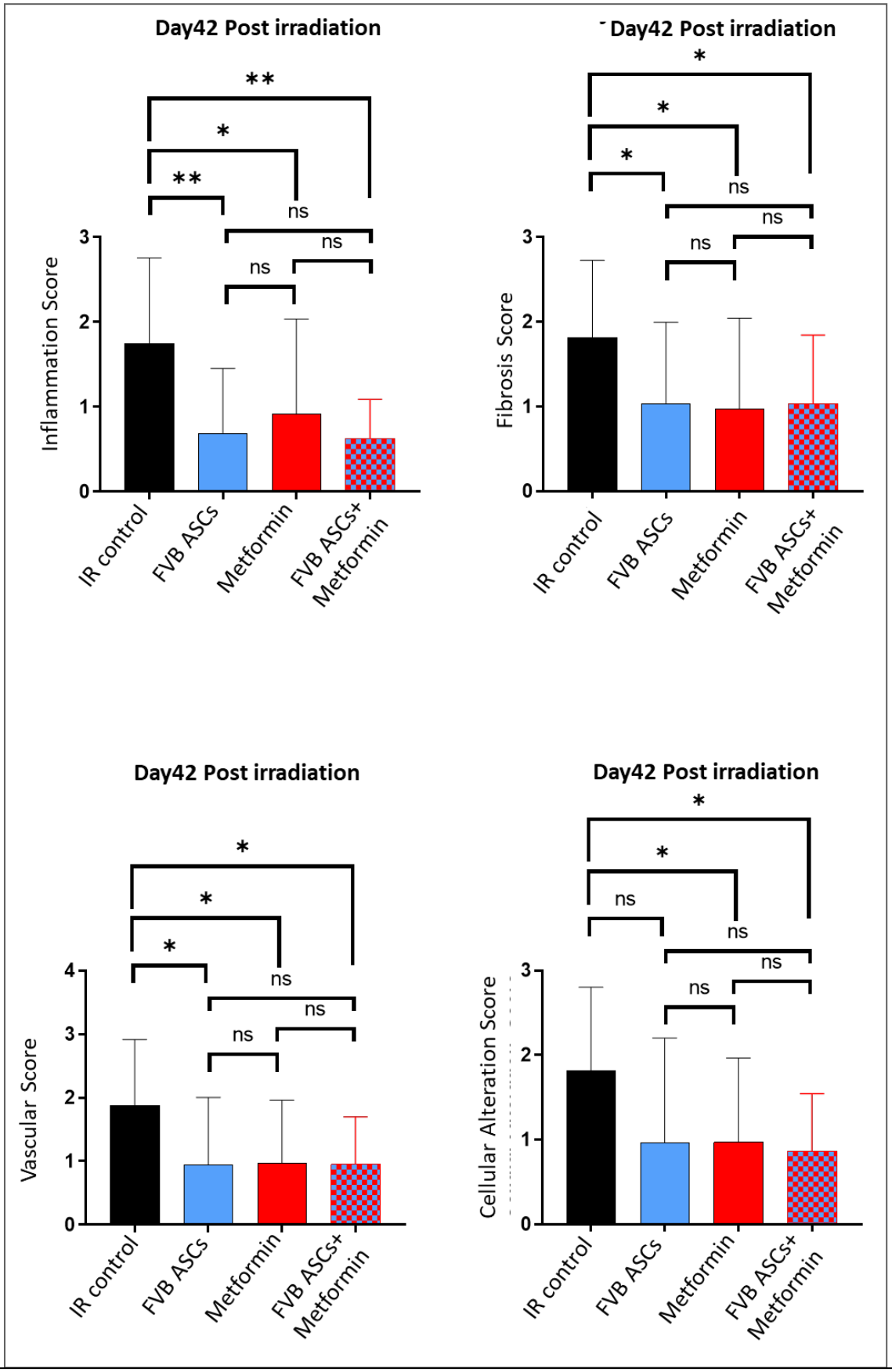

Figure 10: Irradiated skin was harvested on day 42 post-irradiation and fixed. Paraffin blocks of fixed tissues were prepared and sectioned. Masson's Trichrome staining of the skin sections was performed and scored for the abovementioned criteria. $p<0.05$=*, $p<0.005$=**, and ns=non-significant.

Work in progress:
Day 14 injection experiments are in progress. In addition, we are currently performing the gene expression analysis of the skin samples from all the above-mentioned experimental conditions and groups.

3.2.4: Establishment of a robust and reproducible model of radiation-induced skin/muscle fibrosis

During this research, we optimized the radiation-induced fibrosis model and established assays for the evaluation of the functional outcome of the fibrosis. The revised manuscript based on this model establishment is currently under review at the Journal JOVE. Below is the revised manuscript draft:

AUTHORS & AFFILIATIONS:
Yusuf Surucu[1#], Fuat B. Bengur[1#], Katherine S. Yang[1], Benjamin K Schilling[1], Jocelyn S Baker[1], Sheeba Shabbir[2], Renee Fisher[3], Michael W. Epperly[3], Joel S. Greenberger[3], J. Peter Rubin[1], Asim Ejaz[1*]

[1] Department of Plastic Surgery, University of Pittsburgh, Pittsburgh, PA, United States.
[2] Department of Forensic Medicine and Toxicology, HBS Medical and Dental College, Islamabad, Pakistan.
[3] Department of Radiation Oncology, University of Pittsburgh Cancer Institute, Pittsburgh, PA, United States.
[*]**Address correspondence to:**
Asim Ejaz Ph.D.
Department of Plastic Surgery,
University of Pittsburgh Medical Center,
3550 Terrace Street, 6B Scaife Hall, Pittsburgh, PA 15261.
Tel.:
fax: +1 412 648 2821
E-mail: ejaza@upmc.edu

[#] Contributed equally
KEYWORDS:
Radiation-induced fibrosis, skin, radiation injury, fibrosis skin model, limb excursion, walking track

SUMMARY:
Here we present a protocol to induce radiation-induced skin fibrosis in mice and evaluate the functional outcome of fibrosis. This paper describes procedures of hind limb skin irradiation and post-irradiation measurement of chronic impairment via limb excursion and gait index. This model can help understand radiation-related skin fibrosis mechanisms and be used in subclinical therapeutic studies.

ABSTRACT:
Radiation-induced skin fibrosis (RISF) can result from a plethora of scenarios including cancer therapy, accidental exposure, or acts of terrorism. Radioactive beams can penetrate organs affecting the skin, muscles, and internal organs. Skin is the first organ to get exposed to radiation and is susceptible to developing hard-to-treat chronic fibrosis. Currently, limited treatment options are showing moderate efficacy in mitigating radiation-related skin fibrosis. A key factor hindering the development of effective countermeasures is the absence of a convenient and robust model possessing translation to humans. Our lab has established a robust and reproducible murine hind limb skin fibrosis model for prophylactic and therapeutic evaluation of possible agents at both functional and molecular levels.
We irradiated the right hind limb using a single dose of 40 grays to induce skin fibrosis. Subjects developed edema and dermatitis in the early stages proceeded by visible skin constriction and fibrosis. Irradiated limbs showed significantly reduced limb range of motion in the following weeks. Gait index was performed as an additional functional assay, which demonstrated the development of skin fibrosis. These non-invasive functional measurements demonstrated reliable readouts for tracing fibrosis progression which is supported by histological analyses. The radiation dose, application, and post-irradiation analyses employed in our model offer a vigorous and reproducible model for studying radiation-induced skin fibrosis and testing the efficacy of therapeutical agents for mitigation.

INTRODUCTION:

The skin is the largest organ of the body that covers and protects from hazards. It has three distinctive layers epidermis, dermis, and hypodermis. Each layer has its unique function; the epidermis prevents dehydration and microbial invasion. The dermis has a rich network of cells, and extracellular matrix, which acts as a foundation by providing tensile strength and elasticity.[3] Also, the dermal layer gives homage to sensory receptors, hair follicles, glands, and vessels for lymphatic and capillary networks. The hypodermis or subcutaneous tissue has a buffering role with its abundance of adipose tissue, contouring the body and distributing mechanical stress.[4] [5,6]

As a result of the linear progressive nature of radiation, skin is the first organ to come in contact with radiation generated as a result of accidents, war, terrorism, or therapeutical application. The threat of such incidents has intensified due to the increased use of radioactive materials in the industry, medical facilities, and military installations.[7] Clinically, radiation damage to the skin is characterized as cutaneous radiation syndrome (CRS), one of four sub-syndromes of acute radiation syndrome (ARS). Skin response to ionizing radiation has important implications for treatment and protection.[8] Additional injuries like burn and trauma combined with radiation injuries further complicate the clinical outcome.[9] The extent of skin exposure to radiation correlates to a point-of-no-return threshold, from which the impairment of other organs' function results in single or multiple organ failure, and ultimately, patient death.[10,11] Cutaneous radiation injury is comprised of an acute and a chronic phase. Acute radiation injury clinically manifests as erythema, skin edema, dermatitis, blistering, epidermal denudation, dry or wet desquamation, ulceration, and changes in the hair and nails. The chronic phase is manifested as dermal atrophy, fibrosis, chronic ulceration, and telangiectasias.[12,13] In general, acute effects are predominately manifested in the epidermis, while chronic effects are most prominent in the dermis. Acute reaction to radiation exposure leads to a marked decrease in mitotic activity within 12 hours of exposure, followed by hyperemia, cell enlargement, vacuolization, nuclear pyknosis, and fragmentation.[6,14]
Radiation doses exceeding 40Gy result in moist desquamation and loss of epidermis, leading to increased susceptibility to infections.[15] In addition, skin exposure to radiation induces cytokine production, triggering an inflammatory immune response in the dermal layer. Prominent inflammatory mediators include interleukins (IL-1, IL-3, IL-5, IL-6, IL-8) and Tumor necrosis factor-α (TNFα).[16] Failure in the resolution of inflammation can eventually result in fibrosis development at the site of radiation injury.[17] Additional physical wounds or thermal injuries further aggravate this fibrotic response, extending through the epidermis and dermis and into the muscle layer.[18] Transforming growth factor-β (TGFβ) is the key cytokine in fibrosis development.[19] Currently, very few treatment options show promising effects, and all have low patient compliance. Further research into the kinetics of cellular and molecular responses of the skin to different radiation doses will improve our understanding of the radiation-induced skin reactions and the development of new therapies.

To improve clinical measurements of radiation-induced injury to the skin and soft tissues, experimental modeling of therapeutic interventions following irradiation is invaluable to this field of study. Both *in vitro* and *in vivo* models of radiation-induced injury have been described, including cell culture models of irradiated endothelial cells[20,21], fibroblasts[22], or keratinocytes[21] and *in vivo* rodent, pig, and non-human primate animal models. Rodents are widely used in radiation research due to their similarities in response to radiation injury to humans and flexibility of genetic manipulation.[23] Radiation dose requirements are higher in rodents than humans when seeking similar clinical outcomes: desquamation, fibrosis, and necrosis.[18,24] Description of scoring criteria to measure the response to radiation has further enhanced the adoption of rodent models of radiation skin injury.[23,25]

Our research team focuses on understanding the mechanism of radiation-induced skin injury and developing therapeutical options. Thus, establishing a robust and reproducible animal model to create radiation insult with high clinical translatability is essential. This work describes our murine model of skin fibrosis with optimized radiation dose and delivery technique. Combining the functional, histological, and molecular readouts, this model can be successfully used to study the mechanism of fibrosis development and investigate new therapeutical options.

PROTOCOL:

Ethical animal use was approved by the Institutional Animal Care and Use Committee (IACUC), which acts in compliance with Animal Welfare Act. Animals were housed in an Association for Assessment and Accreditation of Laboratory Animal Care International

(AAALAC) approved facility and treated according to the National Institutes of Health Guide for the Care and Use of Laboratory Animals.

1. Anesthesia

1.1. Place mice in the box of a small animal anesthesia system (Figure 1).
1.2. Deliver 4% isoflurane to the box.
1.3. Wait for 5-10 minutes.
1.4. Confirm the anesthesia depth via toe pinch.
1.5. Apply eye lubricant to prevent dehydration.
1.6. Move the subject to the nose cone with 2% isoflurane flow (Figure 4A).
1.7. Use the above technique to anesthetize each mouse for shaving and limb measurement assay.
1.8. Use intraperitoneal pentobarbital injection dose of 1.25 mg/kg to anesthetize mice for irradiation.

2. Euthanasia

2.1. Transfer the subject to a CO_2 line connected box.
2.2. Start the CO2 infusion to reach 30-70% concentration within the chamber.
2.3. For a 5 L chamber, the gas infusion must be between 1.5 - 3.5 liters per minute.
2.4. Wait for the animal to cease respiration for 5 to 10 minutes.
2.5. Euthanase by cervical dislocation via holding the head in place from the skull base and firmly pulling the tail.[26]

3. Skin Area Preparation

3.1. Plan for shaving the mice 2-3 days before irradiating.
3.2. Trim the hairs using a clipper (Figure 2A).
3.3. Apply depilatory cream and wait for 1-2 minutes (Figure 2B).
3.4. Wipe the cream with dry gauze and rinse the skin with phosphate buffer saline (PBS) soaked gauze (Figure 2C).

4. Irradiation Procedure

4.1. Anesthetize each mouse with intraperitoneal injection 5 minutes before irradiation.
4.2. Position the limb in the radiation field (2 x 2cm) and secure it with surgical tape (Figures 3A, B, and C).
4.3. Restrict the body using surgical tape (Figure 3D).
4.4. Place a 3 cm thick bolus to prevent/minimize deep penetration of radiations (Figure 3E).
4.5. Calculate applicator and cutout factors to deliver 40 Gy to the mouse skin.
4.6. We use a linear accelerator to generate a 6-MeV electron beam for 99 seconds to induce β-irradiation burns. In this setting, 25x25 cm applicator area, 1,000 MU/minute dose, and 100 cm distance are enough to deliver 40 Gy.

5. Visual Monitoring of Fibrosis Development

5.1. Use a handheld digital camera to document the progression of fibrosis.
5.2. Use a macro setting to capture detailed photos.
5.3. Take the pictures by positioning the lens closer to the skin and press capture.
5.4. Try to keep the photos as consistent as possible.

6. Measurement of leg excursion as a functional outcome of fibrosis

6.1. Initiate and maintain the anesthesia as described above.
6.2. Prepare a field in front of the nose cone and fix a protractor with tape in the center (Figure 4A).
6.3. Transfer the mouse to the field and gently place its nose on the cone.
6.4. Position the right knee to the protractor's center (Figure 4B).
6.5. Keep the knee fixed with a left hand and use the right hand to dorsiflex the foot with the index and pollex fingers (Figure 4C, 4D).
6.6. Note the degree of extension via reading the value indicated by toes.
6.7. Perform the same procedure on the contralateral non-irradiated leg.

7. Measurement of Gait Functional Index

7.1. The rodent walking track was 3D printed to create a 40 cm walking path suspended at 15 cm with a transparent floor (Figure 5).
7.2. Place a video recorder underneath the track and start filming.
7.3. Open one end of the track and transfer the mouse inside.
7.4. Let the animal walk freely on the track.
7.5. Capture the animal walking as smoothly as possible at least three times.
7.6. Check the quality of the video before recording the next mouse.
7.7. Transfer videos to a computer having a video player, screenshot application, an image processing program, and spreadsheet software.
7.8. Watch the recordings to capture three different, clear footprints via screenshotting (Figure 6).

Open image processing program for toe spread measurements. Select "file" from the upper panel and click "open" to find and display the image to analyze.

7.10. Select "straight line tool" from the second row of the upper panel (Figure 7_1). Using this tool, mark the wall width and click "analyze, set scale" then enter the exact value to "known distance" to calibrate the scale (Figure 7_2, 7_3, 7_4, 7_5).

7.11. Use the "straight line tool" to mark the footprint for different measurements (Figure 6C, 6D; 1: foot length, 2: outer toe spread, 3: inner toe spread) and select "analyze, measure" and record the length value (Figure 8).

Perform the analyses for both irradiated and non-irradiated limbs.

Use the following equation to assess the functionality.[27]

$$FI = 118.9\left(\frac{ETS-NTS}{NTS}\right) - 51.2\left(\frac{EPL-NP}{NPL}\right) - 7.5$$

E = Experimental or injured paw
N = Normal or uninjured paw
TS = toe spread
PL = print length

8. Histology

8.1. Collect tissue samples using pair of sharp scissors.
8.2. Dissect the irradiated skin area by excising a 2 x 1 cm rectangular tissue piece.
8.3. Fix the tissue in 10% Formalin buffered saline.
8.4. Process the fixed tissue for preparing histological sections on slides.
8.5. Stain the slides for hematoxylin and eosin(H&E) stain and Masson's Trichrome stain.
8.6. Visualize the stained slides under a microscope and take images using 10X magnification.

9. Statistics

9.1. Present the data as mean ± standard deviation.
9.2. Evaluate the results using analysis of variance (ANOVA) followed by Bonferroni's multi-comparison test or Student t-test.

Representative Results:

The establishment and optimization of the current irradiation protocol resulted in a consistent and reproducible induction of fibrosis in mice. The mice's right limbs were positioned and secured within the radiation field on irradiation day, and 40Gy was administered.

The development of functional impairment in the skin was monitored by capturing images each week post-irradiation. Photos showed that our optimized protocol could create fibrosis by day 40 with 95% confidence. An example of fibrosis progression elucidated by a visible constriction of the irradiated skin is shown in figure 9. Function impairment is one of the prominent features of radiation-induced fibrosis; as the fibrosis progress, excessive extracellular matrix results in skin constriction and thickening. In addition, radiation-induced fibrosis affects the function of the adjacent muscle. We established a knee extension and video-based toe spread assays to assess limb function quantitatively. Application of 40Gy irradiation dose results in a significant

decrease in the excursion of the irradiated leg compared to the contralateral non-irradiated leg by day 21 post-irradiation (Figure 10). This early result is predominantly related to acute reactions such as edema and dermatitis. Over time, earlier reactions subsided, and the range of motion improved but remained significantly lower than the baseline due to fibrosis. Our group usually performs this analysis up to 42 days post-irradiation (Figure 10).

Improving tissue function is one of the primary goals of therapeutic agents against radiation-induced fibrosis. To further strengthen the clinical relevance of our model, we established a video-based toe spread assay. The steps for this assay are explained above in the protocol section. Irradiation of limbs results in a significant decrease in paw length and toe spread (Figure 11A, 11B). In addition, the calculation of the functional index of the irradiated limb indicated a decrease in limb function (Figure 11C).

Our functional assays are non-invasive and reflect a loss of tissue function post-irradiation attributed to underlying fibrosis developed as a result of irradiation. To draw a conclusive correlation between our functional assay outcome and fibrosis, we performed histological analyses of skin tissue 42 days post-irradiation. Hematoxylin and eosin (H&E) staining of irradiated skin sections revealed a severely hyperplastic epidermis having deep rete pegs and the presence of parakeratotic crusts on the epithelial surface (Figure 12, upper panel). Masson's Trichrome staining showed excessive matrix deposition, thickened epithelium, and denser connective tissue compared to non-irradiated skin sections. (Figure 12, lower panel). In conclusion, our functional test combined with histological analysis confirmed the successful induction and functional evaluation of radiation-induced fibrosis in mice.

FIGURE LEGENDS:

Figure 1: Small animal anesthesia system. Image of the small animal anesthesia system that can be used to anesthetize mice for different procedures.

Figure 2: Pre-irradiation Prep.

A: Trimmed mouse. A representative mouse after hair trimming.

B: Mouse hair removal. Application of depilatory cream to remove hairs.

C: Hair-free limb. A representative hair-free mouse preparation before irradiation.

Figure 3: Hind limb irradiation setup.

A: Radiation field.

B: Limb abduction and body positioning.

C: Limb fixation.

D: Body fixation.

E: Bolus placement.

Figure 4: Limb excursion measurement.

A: Set up for measuring limb excursion. Image showing the arrangement of protractor and anesthesia nose cone for performing the limb excursion measurement.

B: Positioning of the mouse for limb excursion measurement. The image is representative of how and where to place the mouse knee relative to the protractor for executing the limb excursion measurements.

C and D: Performance of mouse limb excursion. Images indicate the positioning of the hand to hold the limb and flexing directions to measure the degree of limb excursion.

Figure 5: 3-D printed mouse walking track. Representative image of 3D printed mouse walking track.

Figure 6: Screenshots of mouse walking pattern. The subject was allowed to walk on the track and captured from beneath.

A: Healthy mice footprint.

B: Irradiated mice footprint.

C: Healthy print measurements. 1: Foot length. 2: Outer toe spread. 3: Inner toe spread.

D: Irradiated print measurements. 1: Foot length. 2: Outer toe spread. 3: Inner toe spread.

Figure 7: Scale calibration with image processing software. This image represents the steps to calibrate the scale. 1: Select straight selection tool, 2: Select a known distance in the photo, 3: Select analyze, 4: Click set scale, 5: Enter known distance.

Figure 8: Measuring distances with image processing software. 1: Select straight selection tool, 2: Select distance, 3: Select analyze, 4: Select measure, 5: Record the distance.

Figure 9: Visual monitoring of fibrosis progression. Images were taken at different time points to monitor the progression from erythema (A: day 3), dermatitis (B: day 9), edema (C: day 14), and fibrosis (D: day 42) following 40 Gy irradiation.

Figure 10: Degree of motion. Representative graph of the change in the degree of limb motion at different time points post-irradiation. ** $p < 0.01$, and *** $p < 0.001$ and **** $p < 0.0001$ as compared with non irradiated control legs.

Figure 11: Mouse walking track analyses.
A: Paw length: Graph representing the change in the paw length at day 42 post-irradiation. * $p < 0.05$ as compared with non irradiated control legs.
B: Toe spread: Graph representing the change in the toe spread at day 42 post-irradiation. **** $p < 0.0001$ as compared with non irradiated control legs.
C: Gait Index: Graph representing calculated gait function index at day 42 post-irradiation.
Figure 12: H&E and Masson's Trichrome Stainings.
Histological sections of non-irradiated health skin and irradiated skin 42 days post-irradiation were stained with Hematoxylin and Eosin (H&E) (upper panel) and Masson's trichrome stain (lower panel). Images were taken using 10X magnification.

Discussion:
Skin injury is a likely outcome of accidental or medical treatment-related exposure to radiation. Nuclear reactors possess an accidental breach risk due to human error or natural disasters like Chernobyl and Fukushima.[28,29] Professional or amateur nuclear devices can be used during an act of terrorism or war. Nevertheless, therapeutical dosing for cancer treatment is the most common exposure, which uses fractionated repeating dose regimens that risk causing radiation-related fibrosis in the treatment area. This common chronic adverse reaction can be prevalent up to 23 percent.[18,30] Therapeutic interventions directed against radiation fibrosis must target the sequential pathological mechanisms involved in different stages of the disease. A cost-effective, reproducible, and translatable small animal model is ideal for further investigations on treatment options and underlying mechanisms. In this protocol, we have explained a murine radiation-induced skin fibrosis model that demonstrates pathological features of skin fibrosis in a translatable manner. Previous studies have shown similarities between the radiation-induced skin reactions and the appearance between humans and mice.[18,23] The availability of a wide variety of strains and the genetically modified models that can help understand the molecular insights and mechanisms of mitigation has made mice an ideal candidate for preclinical research. In addition, the radiation skin working group judged mouse models as the most rational first species for the screening studies.[18]
We administered a single dose of 40 Gy to irradiate the hind limb of mice to create fibrosis in 42 days. Hind limbs can be abducted to have isolated radiation areas; this is highly important because pelvic or abdominal radiation can be fatal. Secondly, mice are less dependent on their hind limbs, which allows us to work with the animals without causing excessive discomfort or fatality. It is crucial to position and restricts the mice to only irradiate hind limbs. Any vital organ radiation will increase fatality, and tail radiation can cause amputation and pain. Irradiation resulted in visible erythema in earlier stages. In humans, erythema marks the earliest phase of the skin reaction to irradiation.[17] Skin pigmentation and black hair color make the detection of erythema difficult; thus, hair removal before irradiation in our mouse model allows better documentation post-irradiation. Radiation dose selection is essential to maintaining the reproducibility of this model. We tested a dose range of 30-45 Gy in our studies, and the results revealed that the pathological effects are inconsistent at lower doses, while higher doses had high mortality. Based on our experience, we decided on a single dose of 40 Gy to be optimal for achieving reproducibility and minimal lethality. Clinical radiotherapy regimens utilize fractioned accumulation of radiation to prevent side effects; replicating this method in animal models could be more relevant. However, the use of fractionated doses in mice does not result in reproducible and clinically similar fibrosis-related pathological features. There are significant differences between mice and humans, yet they are highly relevant in radiation response in the skin.[18,31] Our histology stainings analysis confirmed that we could achieve characteristics of radiation fibrosis comparable in humans with our single-dose murine model. We observed epithelial thickness and an increase in dermal ECM deposition upon irradiation. In scenarios of accidental radiation events, exposure to doses ranging from 20-50 Gy from the fallout is possible. Due to the excess of the cellular papilla, mouse skin usually requires double the radiation dose to have a comparable clinical outcome to human skin. Combined thermal or mechanical trauma can further complicate the healing process and boost fibrosis. Additional mouse models involving a combination injury must be investigated to mimic the accidental or war scenarios. Bolus placement focuses the radiation dose on the skin and reduces penetration to the bone and muscle. In the absence of bolus, we observed more severe effects in limb function

and higher mice lethality rate. This observation correlates with the real-world clinical scenario, "point of no return" extensive skin damage impairs the function of other organs and organ systems.[11,32]

Skin contracture and muscle and nerve injury due to late-stage fibrosis significantly reduce patients' life quality. Our mouse model includes measuring limb excursion and gait function as a functional readout of fibrosis. Limb motion range is significantly reduced after irradiation. The use of a range of motion is a well-accepted endpoint readout of the clinical outcome of fibrotic contracture.[33] In humans, late-stage fibrosis can develop within a couple of months to several years. In our study, earlier effects of radiation caused excessive restriction, yet they resolved with time. Contrarily, late effects such as fibrosis remained unresolved and were prominent in visual, functional, and histological assessments. Genual restriction persisted up to, day 46, our furthest experimental measurement and sacrifice time point.

Walking track analysis has been reliably used to determine the functional recovery from nerve injury-related muscular function. It is a direct readout of functional capacity.[27] The sciatic nerve defect results in defective plantar flexion represented as extended print length and reduced toe spread. The posterior tibial nerve defect representation is similar to the sciatic nerve defect, while the peroneal defect in mice is not well presented compared to the rats.[27] Commonly used technique includes ink-soaked footprints, which can be hard to control and clumsy. We modified the original protocol to use a transparent walking track, recorded mice stroll, took snapshots of paw impression, and measured the toe spread and palm length with an image processing program.

Toe spread and a gait index was added to corroborate the results obtained from the limb excursion assay. Plotting the values of the toe spread and palm length or calculating the gait functional index using the values calculated by Inserra et al.[34] for the sciatic functional index. We observed that irradiation results in a significant decrease in these indices correlating to the loss of limb excursion. In conclusion, walking track analysis can be confidently used to measure limb function in

Irradiated skin can be excised post sacrifice and processed for histological and molecular analyses. Histologically, the skin sections can be stained with hematoxylin & eosin and Masson's Trichrome stain to ascertain inflammation and extracellular matrix deposition. In addition, collagen and elastin-based immune staining can be used to evaluate deposition. For more mechanistic studies, immunohistological analyses can also analyze proteins of interest. Lastly, tissue can be analyzed for gene expression using real-time quantitative PCR or protein expression using either ELISA technique or Multiplex Luminex assay. Supporting cumulative observations showed that our defined protocol could be confidently used to study radiation injuries and assess therapeutics' effects.

Disclosures:

The authors have no competing financial interests or other conflicts of interest related to this work.

Acknowledgments:

This work is funded by research grants from the Department of Defense W81XWH-19-PRMRP-DA, NIAID/NIH Grant 5R21AI153971-02, and PSF/MTF Grant 603902.

Fig 1 Anesthesia Machine

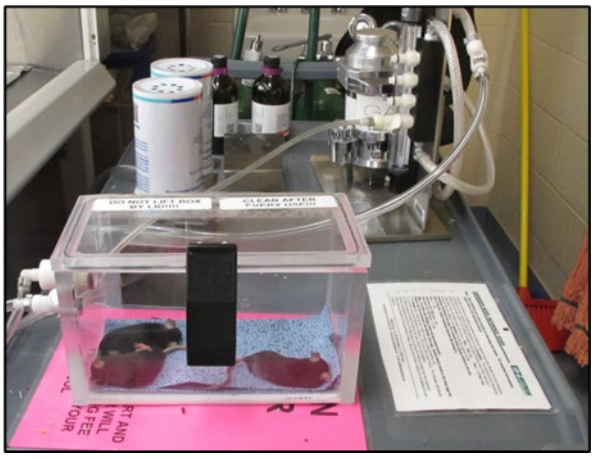

Fig 2

Pre-radiation Prep

Fig 3

Radiation Setup

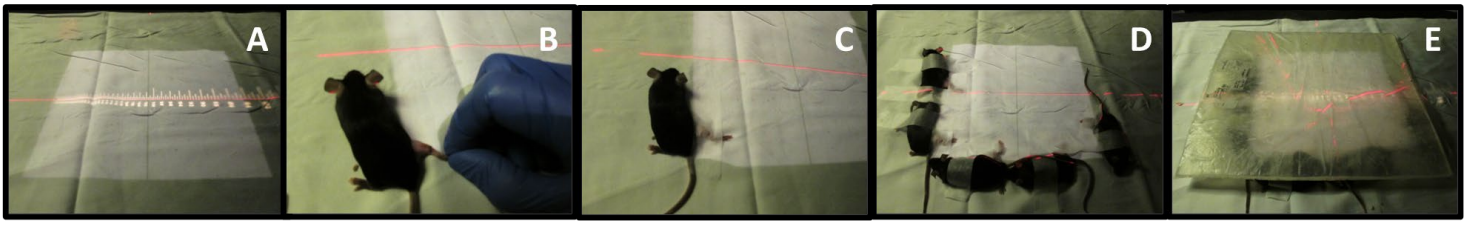

Fig 4

Limb excursion measurement

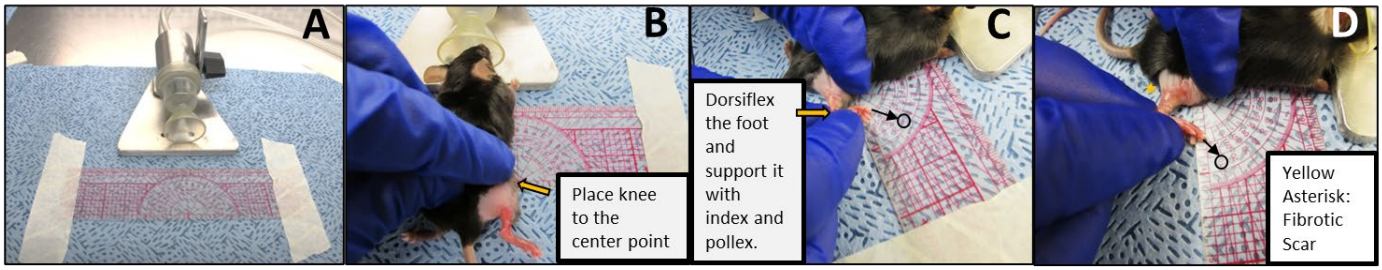

Fig 5

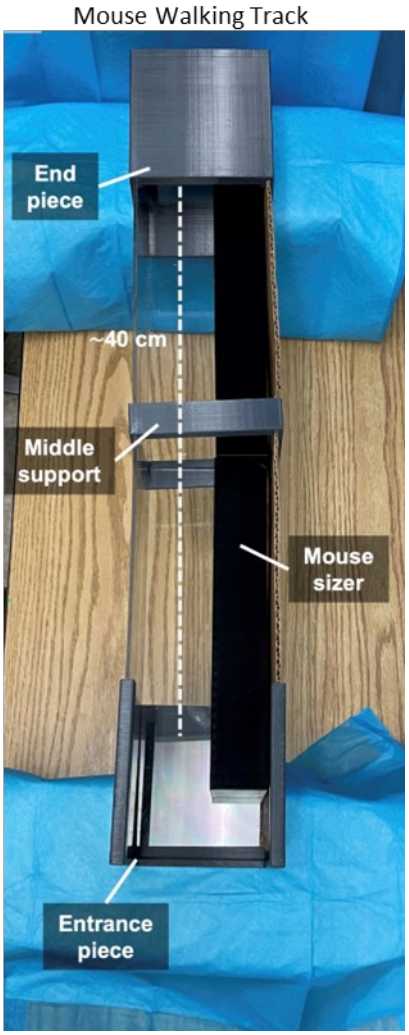
Mouse Walking Track
End piece
~40 cm
Middle support
Mouse sizer
Entrance piece

Fig 6

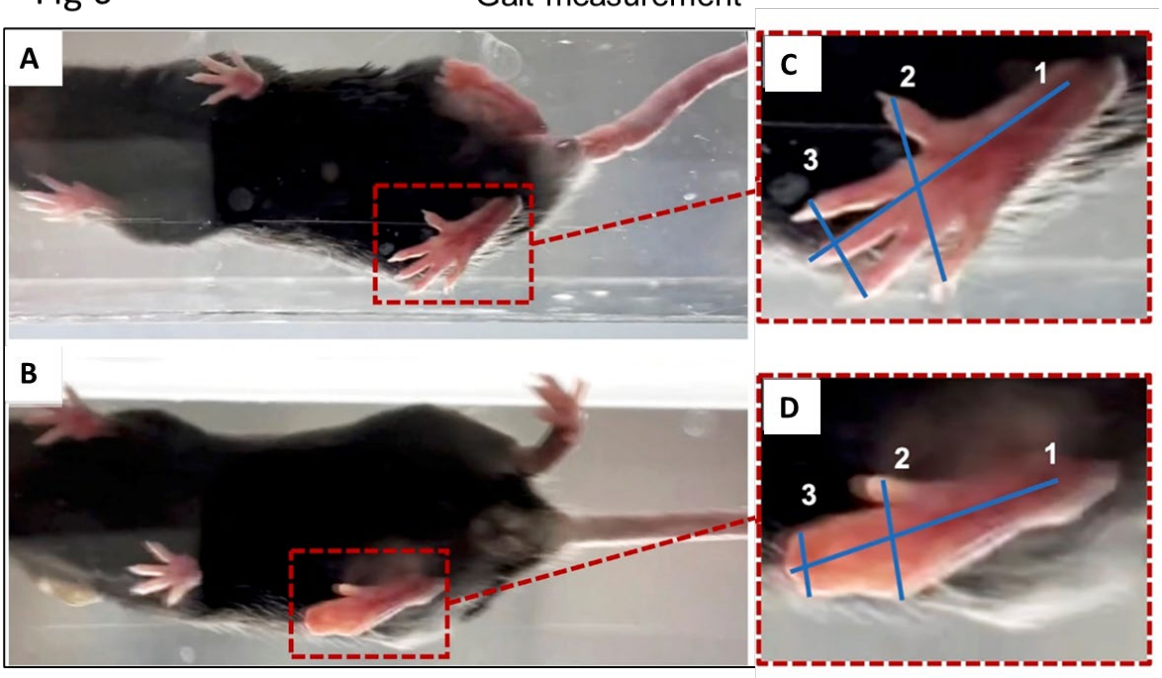
Gait measurement
A
B
C
D
1
2
3
1
2
3

Fig 7 Scale Settings

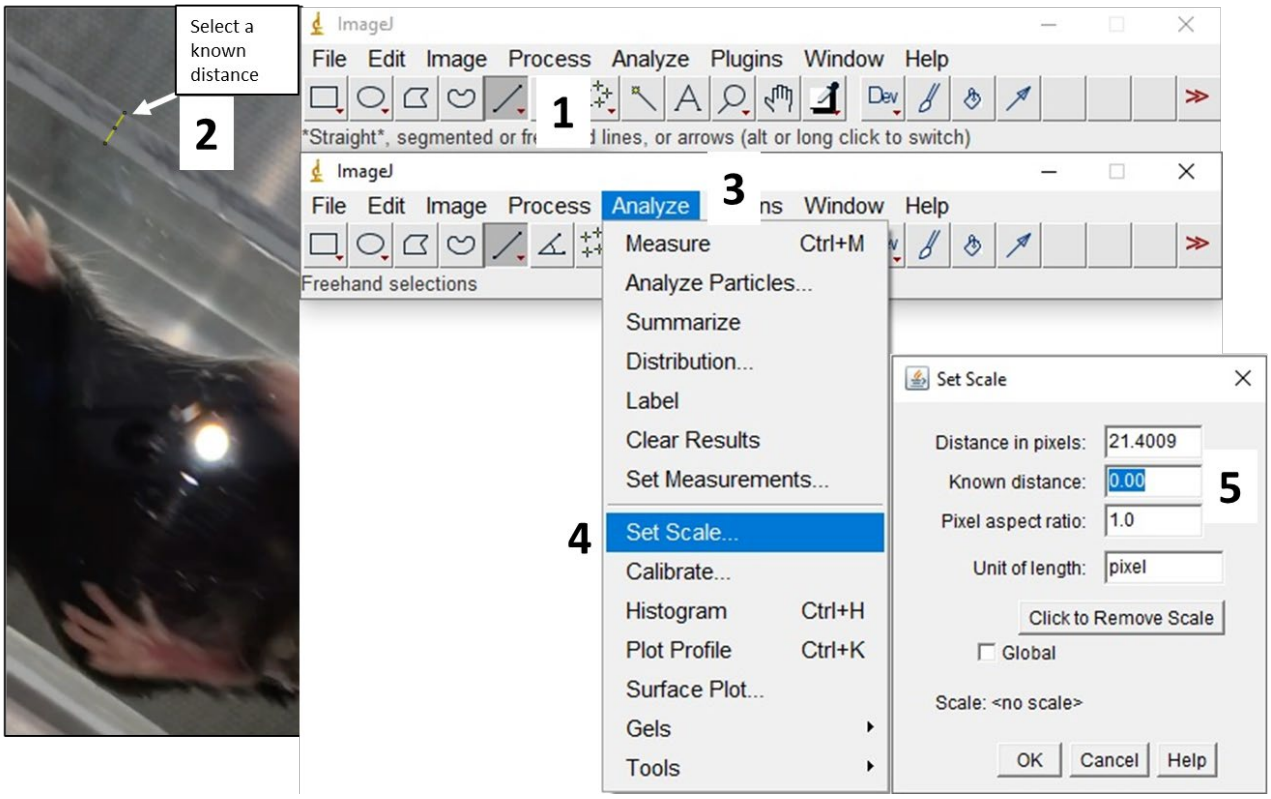

Fig 8 Measuring Points

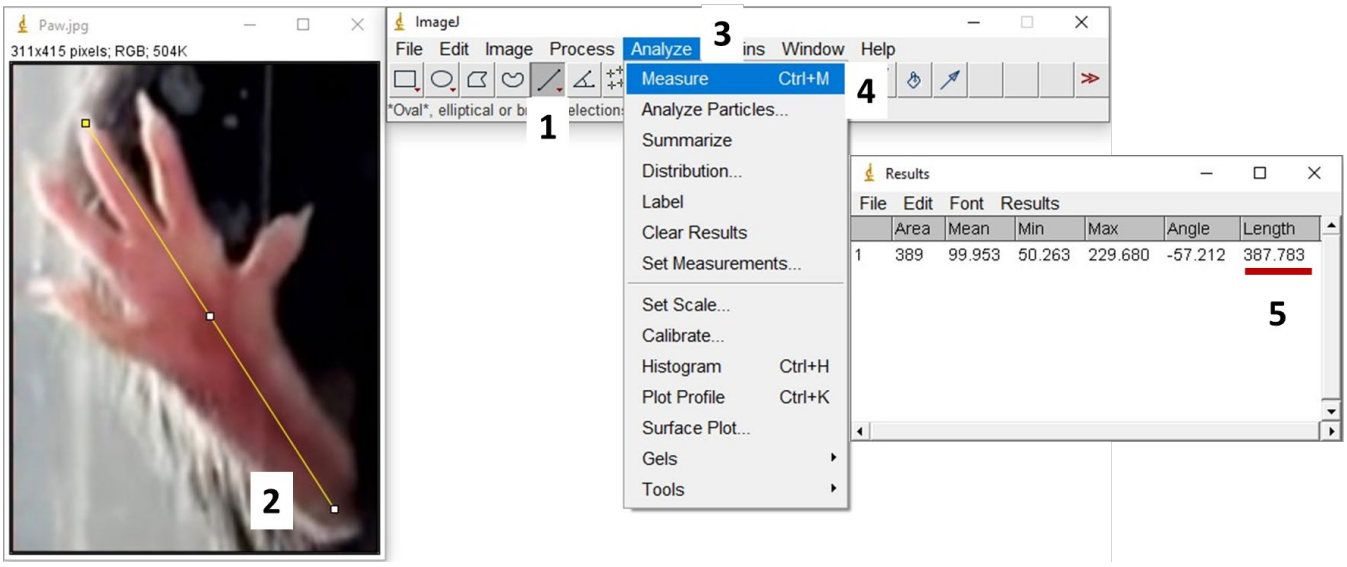

Fig 9

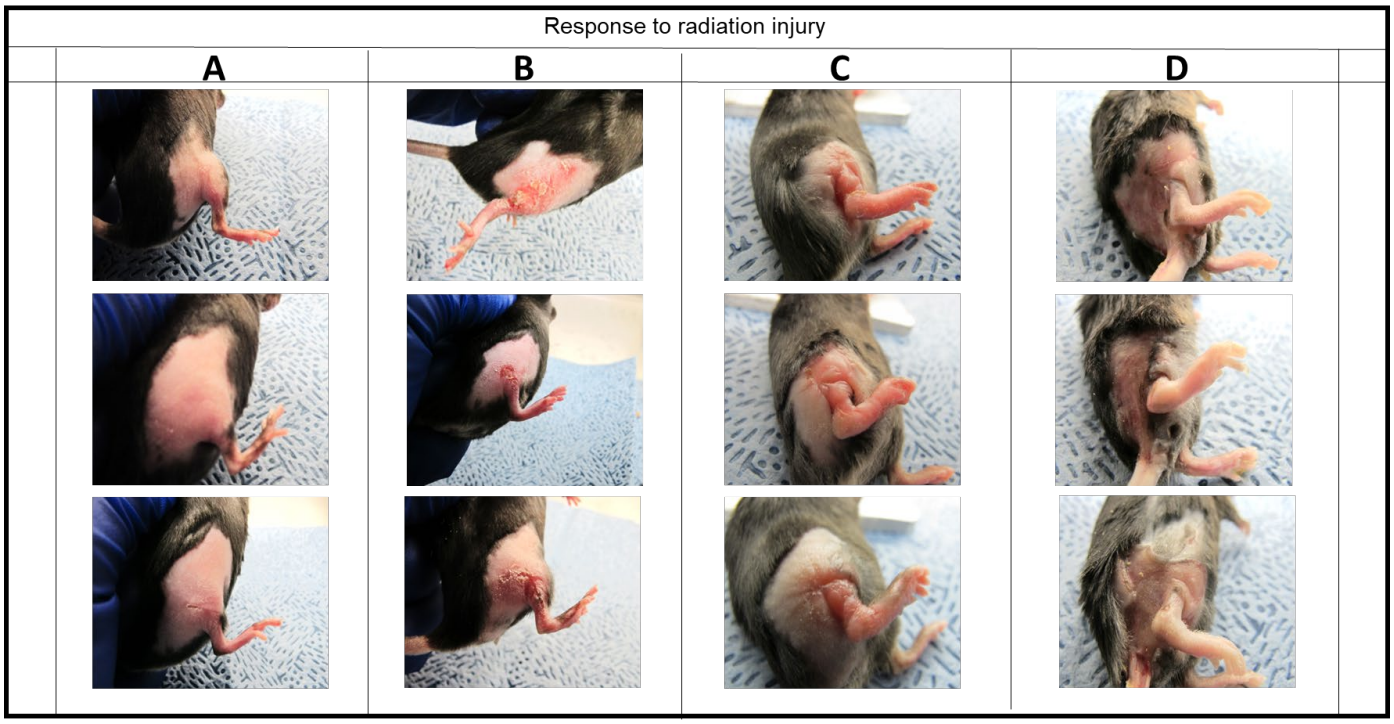
Response to radiation injury
A
B
C
D

Fig 10

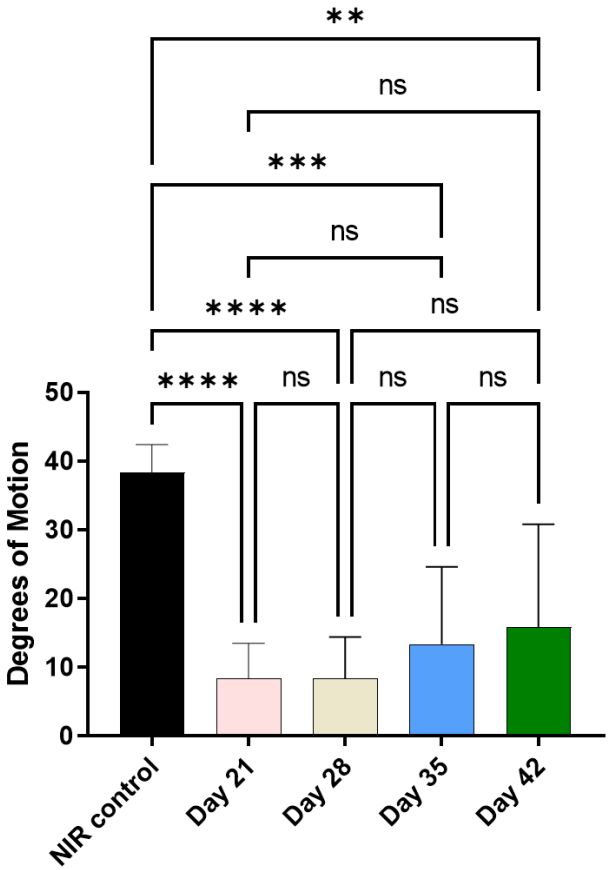
**
ns
***
ns
****
ns
****
ns
ns
ns
Degrees of Motion
50
40
30
20
10
0
NIR control
Day 21
Day 28
Day 35
Day 42

Fig 11

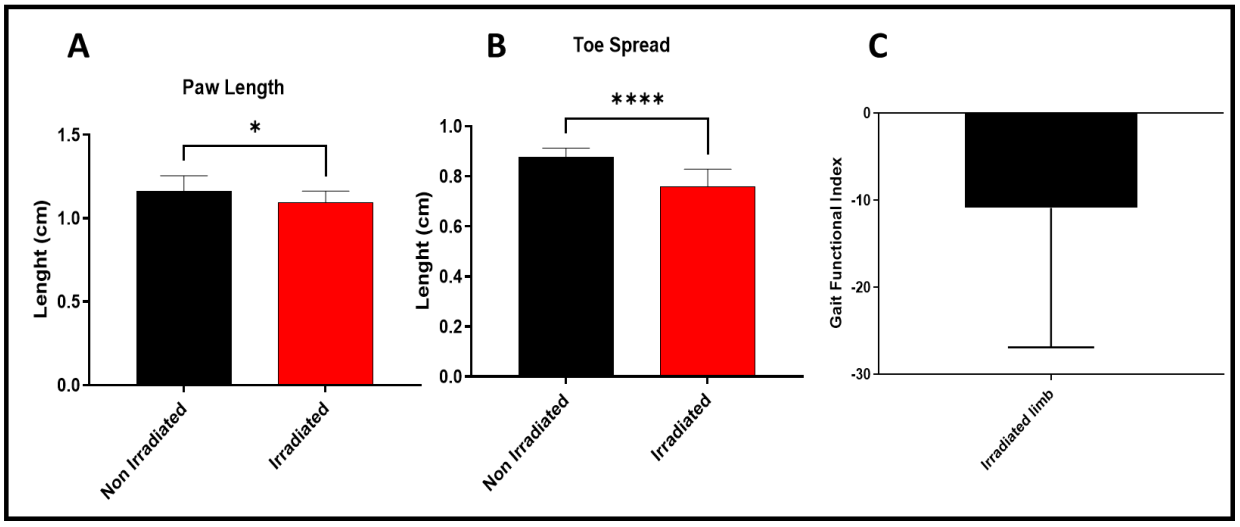

Fig 12

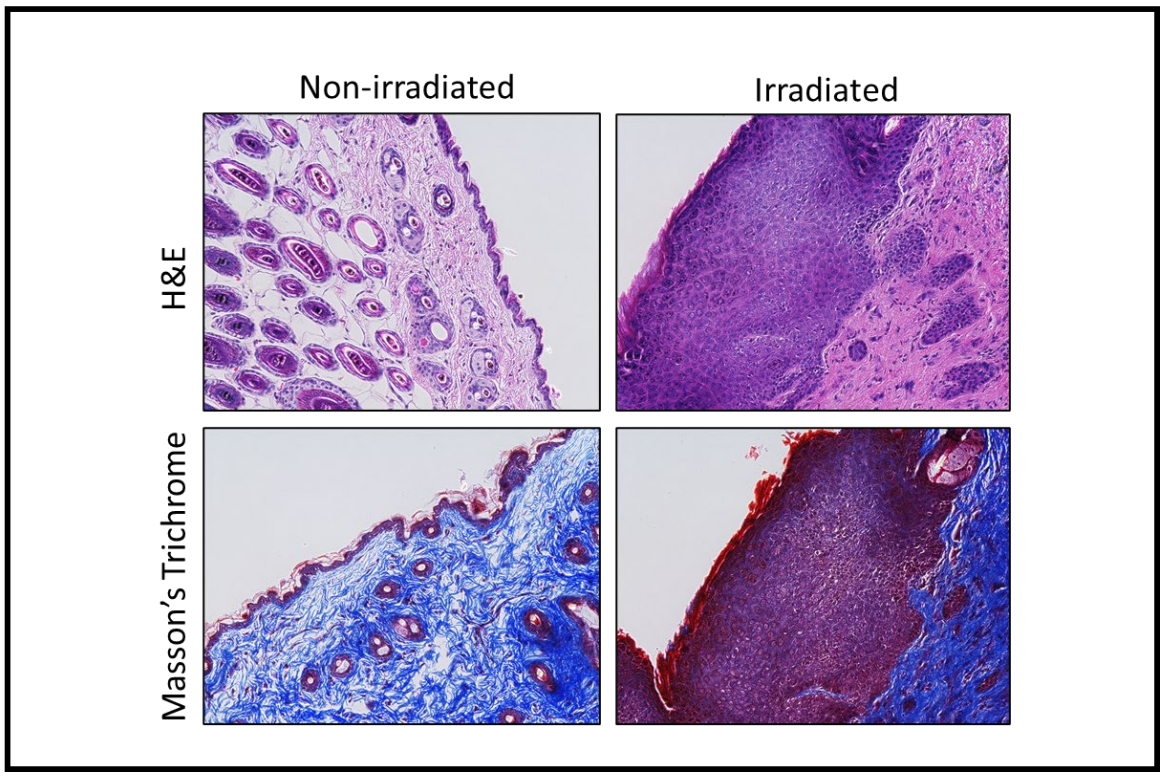

3.2.5: Mechanistic studies

Work in progress: We will be performing further in vitro mechanistic studies to analyze the effect of combination therapy on irradiated cells.

3.2.5. Opportunities for training and professional development:
This grant opportunity has provided the PI (Asim Ejaz Ph.D.) the opportunity to develop as an independent researcher. The award of this grant was followed by an award from the National Institute of Health to develop a human skin culture model to study the effects of radiation injuries in vitro. This award has also helped the PI to achieve an independent tenure track position at the Department of Plastic Surgery, University of Pittsburgh. During the funding period, the PI has been able to publish a study using allogeneic stem cells for treating acute radiation syndrome as a corresponding author in a very well reputed journal Stem Cells translational medicine. In addition, the mechanistic studies proposed in the grant were recently published under the title “Metformin improves stemness of human adipose derived stem cells by downmodulation of mechanistic target of rapamycin (mTOR) and extracellular signal-regulated kinase (ERK) signaling”. In addition, the mouse irradiation model was established and used to fulfill the tasks proposed for this grant. This method is currently under review at Journal JOVE.
Dr. Somaiah Chinnapaka Ph.D. worked on this grant. He was a post-doc in PI’s lab. This award has significantly helped his training and provided him the opportunity to learn new techniques and establish himself as an independent researcher in the field of cellular therapeutics. Currently Yusuf Surucu MD is working as a post-doc and getting the training in PI’s lab. He has contributed significantly to the establishment of the mouse model.

3.2.6. Results dissemination to communities of interest:
Results have been disseminated through publications[35,36] and we will continue to disseminate the results in form of publications and conference presentations.

3.2.7. Plan of work during the next reporting period:
We will continue to work on the tasks as proposed in the SOW. Our working routine has faced a lot of challenges due to COVID-19-related restrictions and a shortage of supplies during the current reporting period. We are hoping that things will get normal in the coming months.

4. Impact
Our published work[35] for the first time has shown the use of allogeneic ASCs as a mitigator of radiation-induced acute syndrome. We consider that this work has set the platform for further investigation of the approach in higher animal models and developing strategies to add allogeneic ASCs to the National Stock Pile for radiation countermeasures.
We showed[36] the beneficial effects of the commonly used drug metformin in improving the health of adipose-derived stem cells. These results showed the effect of combining these two therapeutic agents what is the central idea of the proposal that a combination of these two agents can have synergistic effects.

Impact on other disciplines
We believe that our work using the metformin or ASCs as a mitigator for radiation fibrosis will result in rapid adaptation of this strategy in radiation oncology clinics.

Impact on technology transfer
Nothing to report

Impact on society beyond science and technology
Nothing to report

5. Changes/problems
We do not foresee any considerable changes in the proposed SOW. The team has enormously suffered in executing the proposed SOW at the hands of COVID-19-related restrictions.

6. Products

Journal publications.

Chinnapaka S, Yang KS, Samadi Y, et al. Allogeneic adipose-derived stem cells mitigate acute radiation syndrome by the rescue of damaged bone marrow cells from apoptosis. *Stem cells translational medicine.* 2021.

Chinnapaka, Somaiah, et al. "Metformin Improves Stemness of Human Adipose-Derived Stem Cells by Downmodulation of Mechanistic Target of Rapamycin (mTOR) and Extracellular Signal-Regulated Kinase (ERK) Signaling." *Biomedicines* 9.12 (2021): 1782.

7. Participants & Other Collaborating Organizations

Not applicable.

8. Special Reporting Requirements

Not applicable.

9. Appendices

https://stemcellsjournals.onlinelibrary.wiley.com/doi/10.1002/sctm.20-0455
https://www.mdpi.com/2227-9059/9/12/1782

References.

1. Gallet P, Phulpin B, Merlin J-L, et al. Long-term alterations of cytokines and growth factors expression in irradiated tissues and relation with histological severity scoring. *PloS one*. 2011;6(12):e29399.
2. Ejaz A, Epperly MW, Hou W, Greenberger JS, Rubin JP. Adipose-derived stem cell therapy ameliorates ionizing irradiation fibrosis via hepatocyte growth factor-mediated transforming growth factor-β downregulation and recruitment of bone marrow cells. *Stem Cells*. 2019;37(6):791-802.
3. Breitkreutz D, Mirancea N, Nischt R. Basement membranes in skin: unique matrix structures with diverse functions? *Histochem Cell Biol*. Jul 2009;132(1):1-10. doi:10.1007/s00418-009-0586-0
4. Kim J-S, Jang H, Bae M-J, et al. Comparison of Skin Injury Induced by β-and γ-irradiation in the Minipig Model. *Journal of Radiation Protection and Research*. 2017;42(4):189-196.
5. Kolarsick PA, Kolarsick MA, Goodwin C. Anatomy and physiology of the skin. *Journal of the Dermatology Nurses' Association*. 2011;3(4):203-213.
6. von Essen CF. Radiation tolerance of the skin. *Acta radiologica: therapy, physics, biology*. 1969;8(4):311-330.
7. Dainiak N, Gent RN, Carr Z, et al. Literature review and global consensus on management of acute radiation syndrome affecting nonhematopoietic organ systems. *Disaster medicine and public health preparedness*. 2011;5(3):183-201.
8. Hopewell J. The skin: its structure and response to ionizing radiation. *International journal of radiation biology*. 1990;57(4):751-773.
9. Flynn DF, Goans RE. Nuclear terrorism: triage and medical management of radiation and combined-injury casualties. *Surgical Clinics*. 2006;86(3):601-636.
10. Peter R. Cutaneous radiation syndrome in multi-organ failure. *The British Journal of Radiology*. 2005;(1):180-184.
11. Meineke V. The role of damage to the cutaneous system in radiation-induced multi-organ failure. *The British Journal of Radiology*. 2005;(1):95-99.
12. Berger M, Christensen D, Lowry P, Jones O, Wiley A. Medical management of radiation injuries: current approaches. *Occupational Medicine*. 2006;56(3):162-172.
13. Ralf UP, Petra G. Management of cutaneous radiation injuries: diagnostic and therapeutic principles of the cutaneous radiation syndrome. *Military medicine*. 2002;167(suppl_1):110-112.
14. Bray FN, Simmons BJ, Wolfson AH, Nouri K. Acute and chronic cutaneous reactions to ionizing radiation therapy. *Dermatology and therapy*. 2016;6(2):185-206.
15. Mendelsohn FA, Divino CM, Reis ED, Kerstein MD. Wound care after radiation therapy. *Advances in skin & wound care*. 2002;15(5):216-224.
16. Peter RU. Diagnosis and treatment of cutaneous radiation injuries. *Radiation treatment and radiation reactions in dermatology*. Springer; 2015:185-188.

17. Ejaz A, Greenberger JS, Rubin PJ. Understanding the mechanism of radiation induced fibrosis and therapy options. *Pharmacology & therapeutics*. 2019:107399.
18. Williams JP, Brown SL, Georges GE, et al. Animal models for medical countermeasures to radiation exposure. *Radiation research*. 2010;173(4):557-578.
19. Ejaz A, Epperly MW, Hou W, Greenberger JS, Rubin JP. Adipose-Derived Stem Cell Therapy Ameliorates Ionizing Irradiation Fibrosis via Hepatocyte Growth Factor-Mediated Transforming Growth Factor-beta Downregulation and Recruitment of Bone Marrow Cells. *Stem Cells*. Jun 2019;37(6):791-802. doi:10.1002/stem.3000
20. Haubner F, Leyh M, Ohmann E, Pohl F, Prantl L, Gassner HG. Effects of external radiation in a co-culture model of endothelial cells and adipose-derived stem cells. *Radiation Oncology*. 2013;8(1):66.
21. Ebrahimian TG, Pouzoulet F, Squiban C, et al. Cell therapy based on adipose tissue-derived stromal cells promotes physiological and pathological wound healing. *Arterioscler Thromb Vasc Biol*. Apr 2009;29(4):503-10. doi:10.1161/atvbaha.108.178962
22. Haubner F, Muschter D, Pohl F, Schreml S, Prantl L, Gassner HG. A co-culture model of fibroblasts and adipose tissue-derived stem cells reveals new insights into impaired wound healing after radiotherapy. *Int J Mol Sci*. 2015;16(11):25947-25958.
23. Urano M, Kenton LA, Kahn J. The effect of hyperthermia on the early and late appearing mouse foot reactions and on the radiation carcinogenesis: effect on the early and late appearing reactions. *International Journal of Radiation Oncology* Biology* Physics*. 1988;15(1):159-166.
24. Law M, Thomlinson R. The pathogenesis of necrosis after radiotherapy. *The British journal of radiology*. 1974;47(562):740.
25. Abe Y, Urano M. Fraction size-dependent acute skin reaction of mice after multiple twice-a-day doses. *International Journal of Radiation Oncology* Biology* Physics*. 1990;18(2):359-364.
26. Suckow. CPSaMA. Chapter 35 Euthanasia. In: Weichbrod RH, Thompson GA, Norton JN, eds. *Management of Animal Care and Use Programs in Research, Education, and Testing*. 2nd ed. CRC Press/Taylor & Francis
© 2018 by Taylor & Francis Group, LLC.; 2018.
27. Inserra MM, Bloch DA, Terris DJ. Functional indices for sciatic, peroneal, and posterior tibial nerve lesions in the mouse. *Microsurgery: Official Journal of the International Microsurgical Society and the European Federation of Societies for Microsurgery*. 1998;18(2):119-124.
28. Yamashita S, Suzuki S, Suzuki S, Shimura H, Saenko V. Lessons from Fukushima: Latest Findings of Thyroid Cancer After the Fukushima Nuclear Power Plant Accident. *Thyroid*. Jan 2018;28(1):11-22. doi:10.1089/thy.2017.0283
29. Cardis E, Howe G, Ron E, et al. Cancer consequences of the Chernobyl accident: 20 years on. *J Radiol Prot*. Jun 2006;26(2):127-40. doi:10.1088/0952-4746/26/2/001
30. Williams NR, Williams S, Kanapathy M, Naderi N, Vavourakis V, Mosahebi A. Radiation-induced fibrosis in breast cancer: A protocol for an observational cross-sectional pilot study for personalised risk estimation and objective assessment. *Int J Surg Protoc*. 2019;14:9-13. doi:10.1016/j.isjp.2019.02.002
31. Urano M, Kenton LA, Kahn J. The effect of hyperthermia on the early and late appearing mouse foot reactions and on the radiation carcinogenesis: effect on the early and late appearing reactions. *Int J Radiat Oncol Biol Phys*. Jul 1988;15(1):159-66. doi:10.1016/0360-3016(88)90361-6
32. Meineke V, Fliedner T. Radiation-induced multi-organ involvement and failure: challenges for radiation accident medical management and future research. *The British Journal of Radiology*. 2005;(1):196-200.
33. Stone HB. Leg contracture in mice: an assay of normal tissue response. *International Journal of Radiation Oncology* Biology* Physics*. 1984;10(7):1053-1061.
34. Inserra MM, Bloch DA, Terris DJ. Functional indices for sciatic, peroneal, and posterior tibial nerve lesions in the mouse. *Microsurgery*. 1998;18(2):119-24. doi:10.1002/(sici)1098-2752(1998)18:2<119::aid-micr10>3.0.co;2-0
35. Chinnapaka S, Yang KS, Samadi Y, et al. Allogeneic adipose-derived stem cells mitigate acute radiation syndrome by the rescue of damaged bone marrow cells from apoptosis. *Stem cells translational medicine*. 2021;
36. Chinnapaka S, Yang KS, Flowers Q, et al. Metformin Improves Stemness of Human Adipose-Derived Stem Cells by Downmodulation of Mechanistic Target of Rapamycin (mTOR) and Extracellular Signal-Regulated Kinase (ERK) Signaling. *Biomedicines*. 2021;9(12):1782.